**ORIGINAL ARTICLE**

# A scenario- and spatial-downscaling-based land-use modeling framework to improve the projections of plausible futures: a case study of the Guangdong–Hong Kong–Macao Greater Bay Area, China

Xiangyun Shi[1] · Takanori Matsui[1] · Chihiro Haga[1] · Takashi Machimura[1] · Shizuka Hashimoto[2,3] · Osamu Saito[3]

## Abstract

Land-use change is a crucial driver for achieving a sustainable future. However, the uncertainties of socioeconomic development could lead to different changes in the future land-use patterns. Using a spatial downscaling framework, this study aims to explore possible land-use patterns that can help achieve sustainable development in the Guangdong–Hong Kong–Macao Greater Bay Area, China (the Greater Bay Area). The framework combines the global Shared Socioeconomic Pathways (SSPs) scenarios with local land planning policies to model land-use changes. First, the Land Change Modeler was used to analyze the land-use changes from 2000 to 2010 and build transition potential submodels each of which demonstrates transition potential of different land-use classes. Second, future projections were made for the "business-as-usual" scenario and five localized SSP scenarios that were downscaled from global scenarios and modified based on the local land planning policy. Hong Kong was considered a typical case in the Greater Bay Area that could be used to demonstrate the application of the projected land-use maps by comparing the biocapacity and ecological footprint and estimating the carbon emissions associated with land use. The results of the future projections of land use made under six future scenarios indicated that there is a significant expansion in the urban area under all the scenarios, with varying degrees of decrease in cropland and forest among the different scenarios. Moreover, a land-use change also led to the change in local biocapacity and carbon emissions. Our analysis indicated that in achieving sustainable development not only urban area and cropland should be involved for consideration but should also cover the balance between all land-use classes, and three policy implications were proposed based on our findings.

---

✉ Xiangyun Shi
xiangyun.shi@ge.see.eng.osaka-u.ac.jp

Takanori Matsui
matsui@see.eng.osaka-u.ac.jp

Chihiro Haga
chihiro.haga@ge.see.eng.osaka-u.ac.jp

Takashi Machimura
mach@see.eng.osaka-u.ac.jp

Shizuka Hashimoto
ahash@mail.ecc.u-tokyo.ac.jp

Osamu Saito
o-saito@iges.or.jp

[1] Division of Sustainable Energy and Environmental Engineering, Graduate School of Engineering, Osaka University, Rm# 413, M3 Building of Sustainable Energy and Environmental Engineering, 2-1, Yamadaoka, Suita, Osaka, Osaka 565-0871, Japan

[2] Department of Ecosystem Studies, The University of Tokyo, 1-1-1 Yayoi, Bunkyo-ku, Tokyo 113-8657, Japan

[3] Institute for Global Environmental Strategies, 2108-11 Kamiyamaguchi, Hayama, Kanagawa 240-0115, Japan

# Introduction

Scenario analysis is widely recognized as a powerful tool for assessing and investigating the changes in social, climatic, and environmental systems (Kok et al. 2019; IPBES 2016a) to support governments in developing strategies to achieve the 17 Sustainable Development Goals (SDGs) and development planning (Allen et al. 2017). For this purpose, multiple scenarios have been created to explore alternative futures. For instance, the shared socioeconomic pathways (SSPs), which were catalyzed by the International Panel on Climate Change (IPCC) (Nakicenovic et al. 2014) in 2010, are comprehensive global frameworks that can make significant advances from the previous scenarios (Estoque et al. 2019) and provide a wide range of information on possible future socioeconomic developments (Van Ruijven et al. 2014; Jones and O'Neill 2016). The SSPs have been developed by climate change research community and describe five different plausible pathways, with varying degrees of mitigation and adaptation potentials (O'Neill et al. 2017; Riahi et al. 2017). The pathways are as follows: SSP1–sustainability (taking the green road); SSP2–middle of the road; SSP3–regional rivalry (a rocky road); SSP4–inequality (a road divided); and SSP5–fossil-fueled development (taking the highway) (O'Neill et al. 2017). SSP1 and SSP5 are relatively optimistic trends with high levels of human development and economic growth, as well as efficient environmental management, whereas SSP3 and SSP4 are relatively pessimistic trends with poor social development and environmental protection (Hausfather 2018) (see O'Neill et al. (2017) for more details on SSPs).

Land use and land cover (LULC), being an important and direct driver of global environmental changes, is crucial for achieving sustainable development (Kindu et al. 2018; Ruben et al. 2020; Wang et al. 2018; Acheampong et al. 2018; Díaz et al. 2020). Thus, the spatio-temporal dynamic analysis and projection of LULC were considered as effective ways to understand the changes in LULC (Lu et al. 2019; IPBES 2016b). Moreover, the SSPs provided LULC scenarios based on several assumptions, such as land productivity, food consumption, and land regulations (Popp et al. 2017), thus enabling the exploration of different land-use changes and their consequences in the context of fundamental future uncertainties (Riahi et al. 2017). Furthermore, there are growing attentions in the SSPs applications to regional and local scales for serving to assist policy makers in developing robust climate change adaptation strategies and national or subnational planning, while also providing researchers working at regional, national, and subnational levels with multiple pathways (Palazzo et al. 2017; Valdivia et al. 2015;

O'Neill et al. 2020). For instance, based on the SSPs, Chen et al. (2020a) used the Global Change Analysis Model and a land-use spatial downscaling model to generate a new global gridded land-use data set. Gomes et al. (2020) used an interdisciplinary approach to develop spatially explicit projections of LULC under various SSPs in the Zona da Mata, Brazil, to help in the regional development and forest conservation planning. Hewitt et al. (2020) used SSP1 and SSP5, which were downscaled from Europe, at a regional level to study the impacts and trade-offs of future land-use changes in Scotland, UK. Wang et al. (2018) analyzed and projected the changes in LULC of the Tokyo metropolitan area, Japan from 2007 to 2037 based on the spatiotemporal simulation and Cellular Automata-Markov Model.

In China, the LULC changes of the past 2 decades have been arguably the most widespread in the history of the country (Yirsaw et al. 2017). Unprecedented urban development poses a huge challenge to sustainable development. Therefore, numerous studies were conducted to project future land-use changes and provide references and suggestions to identify sustainable pathways and make policy decisions (Chu et al. 2018; Song et al. 2020; Lin et al. 2020; Dong et al. 2018). For instance, Liu et al. (2017) proposed a future land-use simulation (FLUS) model to simulate multiple land-use scenarios in China. Liao et al. (2020) performed land-use simulations using the FLUS model under plant functional type classification in the context of various SSPs in China. Chen et al. (2019b) combined an urban growth simulation model with a multiregion input–output model to explore the teleconnections between the future urban growth of China and its impacts on the ecosystem services under different SSPs. However, the previous land-use projections related to China were performed on a national/provincial scale, with medium to coarse resolution (e.g., $1 \times 1$ km$^2$) (Dong et al. 2018; He et al. 2017). As these land-use projections made with a coarse resolution can lead to an underestimation of the influence of urbanization (Liao et al. 2020), a downscaled simulation at a higher resolution was required.

Thus, this study aimed to project the future land-use patterns at a higher resolution to explore the SSPs implications and the possible land-use changes caused by urban development on SDG 11: sustainable cities and communities. For this purpose, we proposed a spatial downscaling framework that couples the global SSPs narratives and local land planning policy using a land change modeling method to simulate the future land-use scenarios.

## Study area

The Guangdong–Hong Kong–Macao Greater Bay Area (Greater Bay Area) was used as the research object for the simulations of future land-use scenarios, it represents one of the most prominent and fastest growing regions of China (Hasan et al. 2020). However, for a long period, the urban development activities in the region have been concentrated in near-shore areas, and the ecosystem of the region has undergone degradation (Li and Wang 2019), such as an ecological deficit, due to an increased ecological footprint (WWF 2019). Therefore, the Greater Bay Area was chosen for a case study. The Greater Bay Area comprises the two special administrative regions, namely, Hong Kong and Macao, and nine municipalities, namely, Guangzhou, Shenzhen, Zhuhai, Zhongshan, Jiangmen, Zhaoqing, Foshan, Huizhou, and Dongguan in the Guangdong Province,
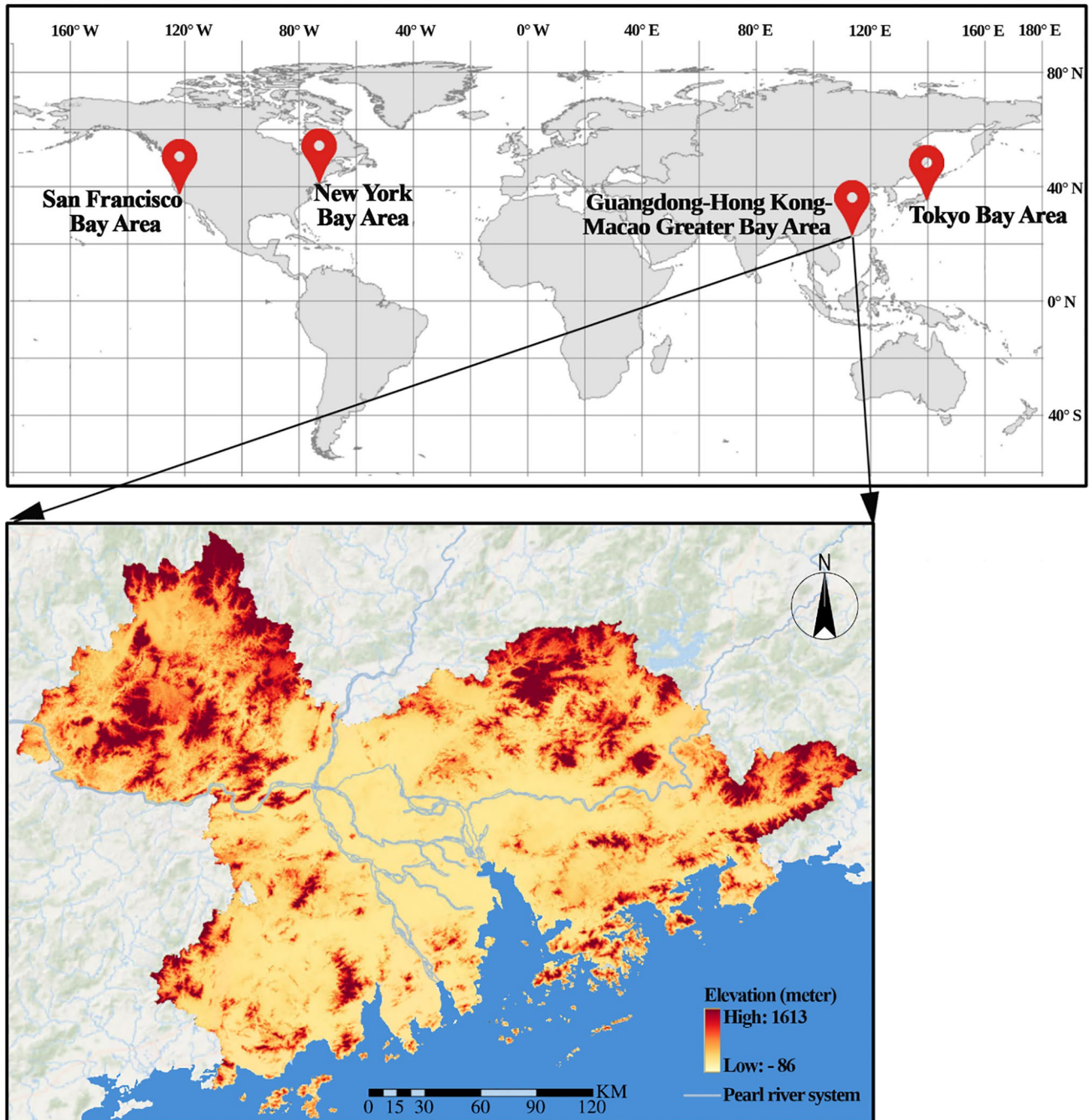


**Fig. 1** Location of the Greater Bay Area, China

covering an area of approximately 56,000 km². Its total population was estimated to be over 71 million by the end of 2018 (Greater Bay Area 2018). The Greater Bay Area is surrounded by mountains on three of its sides and is bordered by the sea on its southern side. Moreover, it has the Pearl River Delta plain at its center (Fig. 1). Most of its area is at an elevation that is less than 200 m above sea level. The Greater Bay Area is the fourth largest bay area in the world, following San Francisco, New York, and Tokyo Bay Areas. Being one of the most open and economically vibrant regions of China, the Greater Bay Area is the key to the strategic planning of the development blueprint of the country and will develop into an international first-class bay area and a world-class city cluster (Central Committee of the Communist Party of China 2019).

In addition, Hong Kong was used as an example to demonstrate the application of the projected land-use maps owing to the fact that it is among the top cities in the world in terms of per capita consumption of goods and resources (WWF 2013). The rapid growth of its population and economy places a heavy burden on land supply, which is being overcome by the reclamation of land from the sea (Asia 2020). In 2018, its total population was 7.48 million (DSEC 2020), and its total land area was approximately 1,110 km². Hong Kong occupies only 1.98% of the Greater Bay Area (Fig. 2), although its population is approximately 10.54% of the total population of the Greater Bay Area. Being a developed and typically high-consumption city of the Greater Bay Area, Hong Kong could be used to demonstrate the sustainable development of cities. Therefore, we have confined our observations to Hong Kong.

## Materials and methods

Figure 3 presents the framework used in the study. The core feature of the framework is the spatial downscaling simulation that can be used in the projections of future land-use scenarios. It combines the global SSPs narratives with the local land planning policy using a land change modeling method. Two types of outcomes were projected using the Land Change Modeler (LCM) software, which is an integrated module of TerrSet 18.31 (Clark labs 2020). One outcome consists of the business-as-usual (BaU) land-use map, which represents the continuation of the past trends in the Greater Bay Area and could be directly generated using its default transition probability matrix without any interventions (Fig. 3). The other outcome represents land-use maps under various global SSPs combined with the local land planning policy and used the 1-km resolution future land-use gridded maps. These maps were projected by Liao et al. (2020) and Li et al. (2016) as initial reference data to adjust the transition probability matrix to generate outcomes at a 300-m resolution, thereby achieving spatial downscaling. Considering the implementation period of the current local land planning policy and roughly the same pattern of population distribution from 2020 to 2030 (Wang et al. 2014), 2030 was selected as the time horizon in the scenario simulations. Furthermore, the nature reserves and future population distribution maps were used as the planning constraints and incentives to further shape the spatially explicit future land-use patterns. Finally, Hong Kong was used as an example to demonstrate the application of the projected land-use maps. The following section describes the reasons for choosing the LCM and its specific operations.
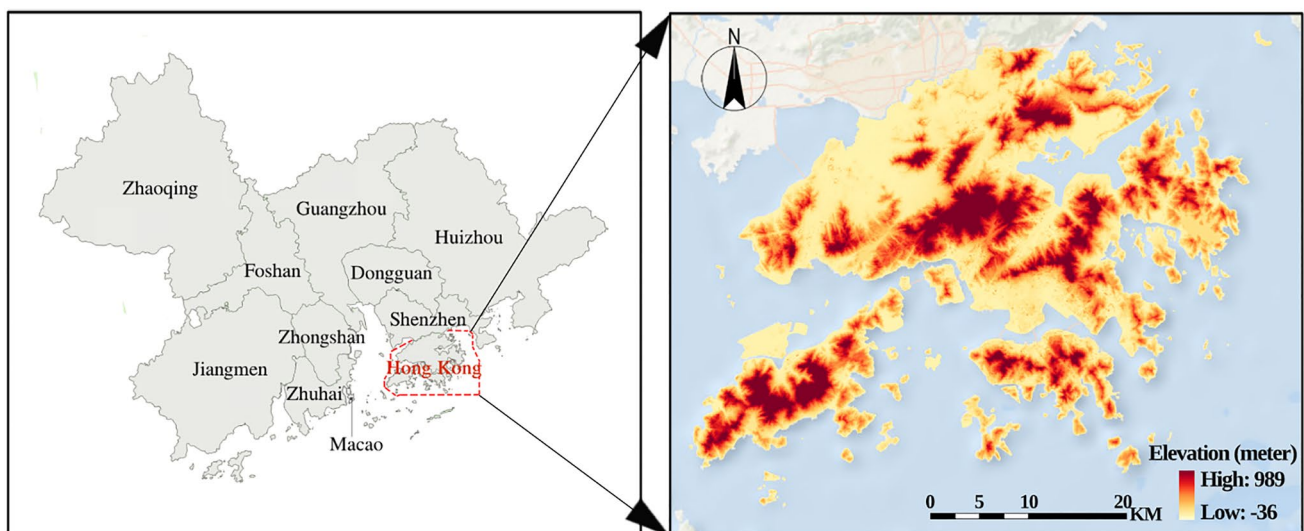


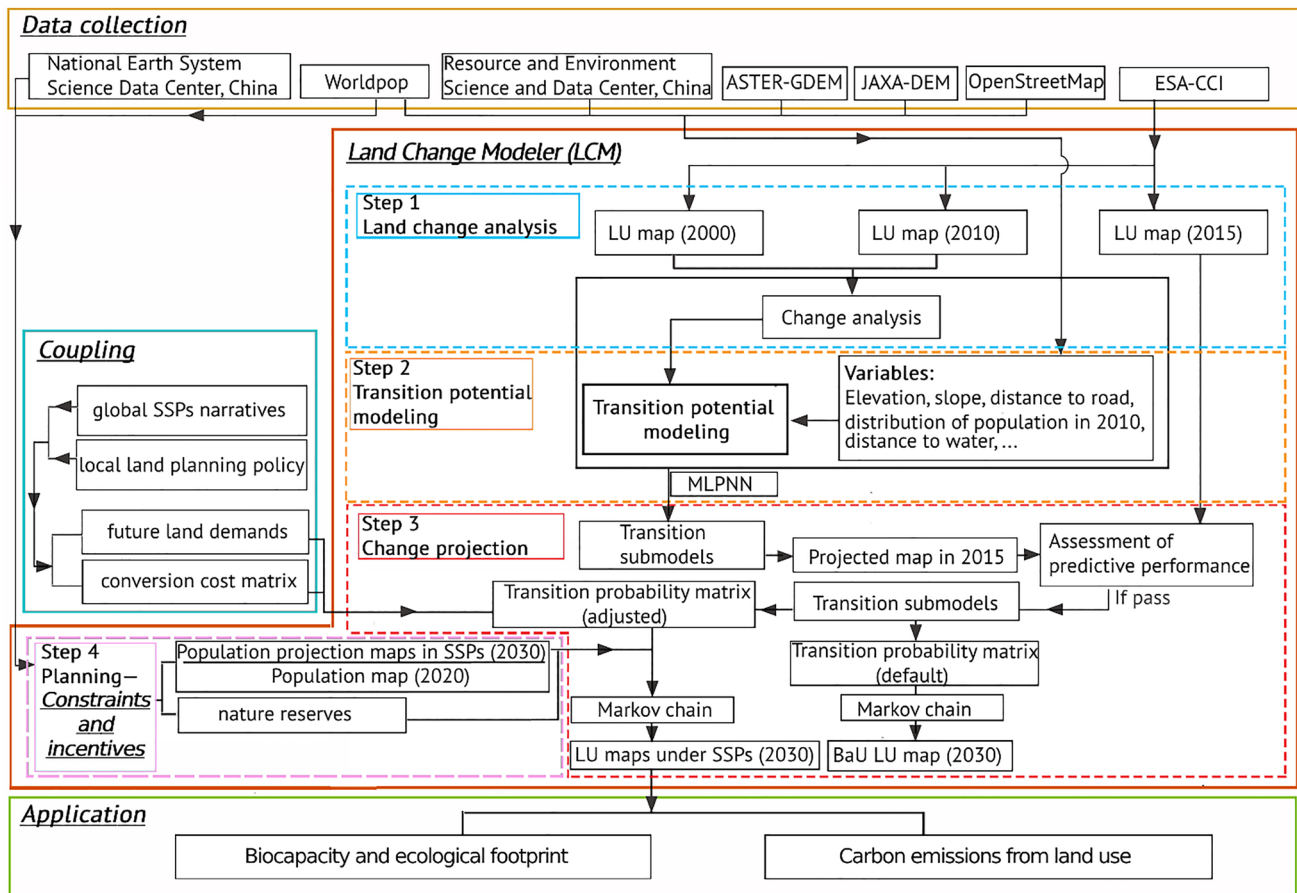**Fig. 2** Location of the Hong Kong Special Administrative Region, China

**Fig. 3** Research framework. LU stands for land use and MLPNN for multilayer perceptron neural network. The yellow, red, cyan, and green solid lines indicate data collection, LCM simulation, coupling of global SSPs narratives with the local planning policy, and applica-tion that is based on projected land-use maps, respectively; the blue, yellow, red, and pink dashed lines denote the four subcomponents of LCM

## LCM

Out of the various methods used for scenario building, the Markov chain modeling is the most common approach used to quantify future changes, particularly in pattern-based models (Rimal et al. 2018; Mas et al. 2018; Vázquez-Quin-tero et al. 2016). The Markov chain modeling calculates the transition areas/probability matrix via cross-tabulation between the land-use categories of two maps (Olmedo and Mas 2018). The LCM is being applied in many disciplines (Eastman and Toledano 2018) and is being widely used to project land-use changes under different future scenarios/land-use policy interventions (Shoyama et al. 2019; Aung et al. 2020). The LCM is an effective and powerful model owing to its Markov chain-based neural network (Hasan et al. 2020; Kumar et al. 2015). Therefore, we selected the LCM (version 18.31) to project the land-use patterns of the Greater Bay Area for 2030. Four major subcomponents of the LCM (Fig. 3) were used: (1) land change analysis, (2)

transition potential modeling, (3) change projection, and (4) planning.

### Step 1: Land change analysis

Two land-use maps of 2000 and 2010 (Fig. 3; Table 1) were utilized in the land change analysis. Six land-use classes were identified, namely, cropland, forest, bush and grass-land, urban area, barren land, and water. The land transi-tions were identified based on the calculated gains and losses of the land-use classes. Land transitions in areas less than 10 km$^2$ in extent were disregarded; only the dominant transi-tions that included 99% of the transitions were used for the modeling.

### Step 2: Transition potential modeling

Two setups of the transition submodels, namely, the sub-model structure and simulation approach, were employed to compute the transition potentials. Initially, 14 potential

**Table 1** Data sources

| Name | Time | Resolution | Organization | Source |
|---|---|---|---|---|
| Land-use and land cover map | 2000, 2010, 2015 | 300 m | ESA-CCI | https://www.esa-landcover-cci.org/?q=node/158 |
| Road map | 2013 | Shape file | OpenStreetMap | https://download.geofabrik.de/ |
| River map | – | Shape file | Resource and Environment Science and Data Center, China | http://www.resdc.cn/data.aspx?DATAID=221 |
| DEM | 2019 | 30 m | ASTER-GDEM; JAXA-DEM | https://ssl.jspacesystems.or.jp/ersdac/GDEM/E/ https://www.eorc.jaxa.jp/ALOS/en/aw3d30/ |
| Nature reserves | 2015 | Shape file | National Earth System Science Data Center, China | http://www.geodata.cn/data/datadetails.html?dataguid=120209853934500&docId=9768 |
| Population map | 2010, 2020 | 100 m | Worldpop | https://www.worldpop.org/geodata/listing?id=69 |
| Population projection maps in SSPs | 2030 | 100 m | Chen et al. (2020b) | |

Due to the fact that the population projection maps of the SSPs that were created by Chen et al. (2020b) do not involve Hong Kong and Macao and based on the data obtained from IIASA (2018), the population projection maps of these two areas were computed using the spatial distribution pattern of the population in 2020. Please refer to supplementary material for more details

**Fig. 4** Variables used for building the submodels of the LCM. Evidence likelihood is effective for incorporating categorical variables into an analysis (Eastman 2015) and can be generated in the variable transformation utility panel of the LCM
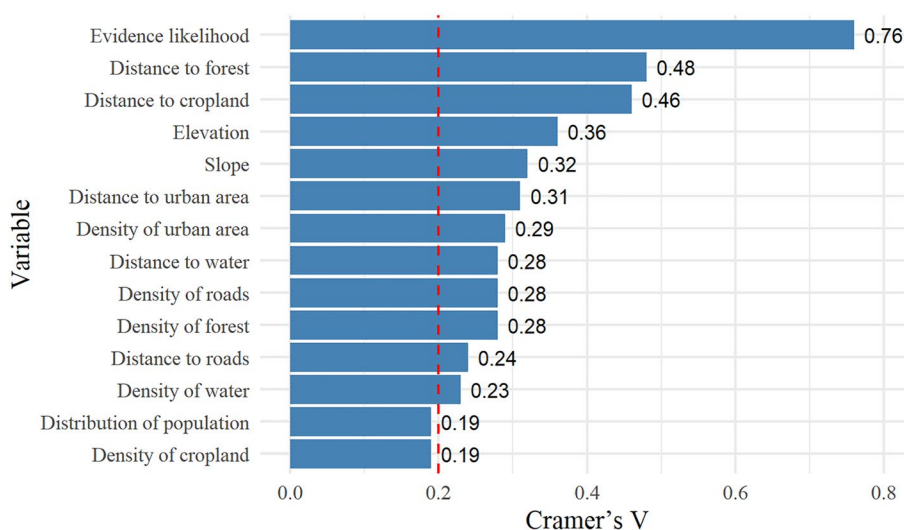


independent drivers (Fig. 4) related to land-use changes were selected. Then, using Cramer's V approach that can measure the association between each driver and each land class, 12 strongly associated variables exceeding 0.2 in value were identified (Hashimoto et al. 2019) to build the submodel structure.

The submodel has three options for the simulation approach, namely, multilayer perceptron neural network (MLPNN), similarity-weighted instance-based machine learning (SimWeight), and logistic regression. However, both the SimWeight and logistic regression approaches can perform only one transition per submodel, whereas the MLPNN can run multiple transitions (up to nine) per submodel (Eastman 2015) and robustly simulate nonlinear relationships (Shoyama et al. 2019). Therefore, the MLPNN

simulation was adopted to model the land-use transitions from 2000 to 2010.

**Step 3: Change projection**

The changing quantity of each transition can be modeled to generate a plausible future land-use map through a Markov chain or specification of the transition probability matrix (Eastman 2015). The BaU case in the present study was generated using the default transition probability matrix without any modifications (Fig. 3). The LCM can produce two modes of change projection, namely, hard and soft projections. A hard projection is a commitment to a specific scenario. Contrarily, soft projection is a continuous mapping of the degree of vulnerability to change in the 0–1 range, with high values indicating high susceptibilities to change. The

soft projection indicates the extent to which an area has the conditions adequate to undergo changes, without showing what exactly will change (Eastman 2015). Therefore, hard projection was adopted to assess the predictive performance under the BaU scenario.

### Step 4: Planning constraints and incentives

The constraints and incentives, which are embedded in the planning subsection of the LCM, can be specified for each of the transitions to enable the integration of change allocation into the projection process thus making the model more robust (Eastman 2015) and can shape the future land-use pattern further. Zero values on the map relate to absolute constraints, values between zero and one to disincentives, values equal to one as no-constraints, and values greater than one to incentives. In the study, two types of maps were considered as the constraints and incentives: (1) the population distribution maps under SSPs were used to create constraint and incentive layer by dividing the future population projection map for 2030 (100 m resolution) (Chen et al. 2020b) by the population distribution map for 2020 (100 m resolution) (Worldpop 2020). The total population of the Greater Bay Area for 2030 was estimated to be 99,575,075 by SSP1; 101,190,772 by SSP2; 102,183,566 by SSP3; 98,826,910 by SSP4; and 99,993,406 by SSP5 (Table 3). In 2020, the population of the area was 63,050,321; (2) the nature reserves in the Greater Bay Area (Table 1) were specified as constraints by assigning a value of zero to indicate that development was not allowed in the areas.

### Correlating land-use modeling with local land planning policy-coupled SSPs

The land transition probability matrix in the LCM could be edited to facilitate future projections and was determined by two key factors (Fig. 3): (1) future land demands and (2) the conversion cost matrix describing the difficulty of converting from the current land-use class to the target class (Dong et al. 2018; Liu et al. 2017). Therefore, land-use modeling and scenarios could be correlated by adjusting the two

factors according to the local land planning policy and SSPs narratives.

First, with regard to the future land demands in the Greater Bay Area under the different SSPs, the studies by Liao et al. (2020), Li et al. (2016), and Li and Chen (2020) were used as the main reference points. Liao et al. (2020) projected the future land-use maps of China at a resolution of 1 km under the plant functional type classification of the SSPs. Therefore, the future areas of forest, urban area, barren land, and water could be calculated directly using the ArcGIS pro (version 2.2) software to extract the Greater Bay Area from China. Furthermore, the policy document named Letter of support for the Guangdong–Hong Kong–Macao Greater Bay Area and Shenzhen to explore the reform of natural resources (People's government of Guangdong province 2020) was introduced by the Ministry of Natural Resources in 2020. It urges the local government to adopt the cultivated land requisition–compensation balance policy to develop built-up land. Accordingly, if the local cultivated land is converted into built-up land, a piece of land of the same size and quality has to be reclaimed in another region for farming, thus guaranteeing the balance of cultivated land throughout the country (The National People's Congress of the PRC 2019). Thus, the demand for cropland was adjusted considering this important policy and according to Li and Chen (2020), who projected the future impacts of the cropland balance policy of China under different SSPs. The bush and grassland area was determined based on the demands for the five land-use classes and the 1-km global land-use data set (Li et al. 2016). In this way, the future land demands for the six land-use classes of the Greater Bay Area could be determined for 2030 (Table 2).

Second, the conversion cost matrix had to be determined in two steps: (1) combining SSPs narratives with local land planning policy to qualitatively determine the difficulty levels of land-use conversion and (2) quantifying those difficulty levels. In the first step, the policy documents named Land Planning of Guangdong Province (Department of Natural Resources of Guangdong Province 2017, 2018) and Letter of support for the Guangdong–Hong Kong–Macao Greater Bay Area and Shenzhen to explore the reform of

**Table 2** Land demands (km$^2$) in the Greater Bay Area in 2030 under each SSPs, categorized according to land-use class

|  | Cropland | Forest | Bush and grassland | Urban area | Barren land | Water |
|---|---|---|---|---|---|---|
| SSP1 | 20,567 | 19,746 | 2,373 | 9,561 | 50 | 3,461 |
| SSP2 | 18,387 | 21,080 | 3,354 | 9,327 | 149 | 3,461 |
| SSP3 | 17,158 | 21,463 | 4,872 | 8,703 | 101 | 3,461 |
| SSP4 | 20,335 | 19,960 | 2,386 | 9,471 | 145 | 3,461 |
| SSP5 | 20,539 | 20,112 | 2,006 | 9,471 | 169 | 3,461 |

The BaU case was generated using the default transition probability matrix in the LCM (Fig. 3 and Step 3), therefore, no extra adjustment of land demand or conversion cost matrix was required for BaU

**Table 3** Overview of land-use narratives and demographic factors of the five SSPs

| | SSP1 Sustainability | SSP2 Middle of the road | SSP3 Regional rivalry | SSP4 Inequality | SSP5 Fossil-fueled development |
|---|---|---|---|---|---|
| **Land-use** | | | | | |
| Land-use change regulation | Strong regulation to avoid environmental disruption | Medium regulation | Limited regulation; continued deforestation | Highly regulated in MICs and HICs; lack of regulation in LICs | Medium regulation |
| Land productivity growth | High improvements in agricultural productivity | Medium pace of technological change | Low technology development | High improvements for large-scale industrial farming; low for small-scale farming | Highly managed, rapid increase in productivity |
| Environmental impact of food consumption | Low growth in food consumption, low-meat | Material-intensive consumption, medium meat consumption | Resource-intensive consumption | Elites: high consumption; Rest: low consumption | Material-intensive consumption, meat-rich diets |
| **Population growth** | | | | | |
| High fertility | Low | Medium | High | High | Low |
| Other low fertility | Low | Medium | High | Medium low | Low |
| Rich low fertility | Medium | Medium | Low | Medium low | High |
| Population projections of the Greater Bay Area in 2030 | 99,575,075 | 101,190,772 | 102,183,566 | 98,826,910 | 99,993,406 |
| **Urbanization level** | | | | | |
| HICs | Fast | Central | Slow | Central | Fast |
| MICs | Fast | Central | Slow | Fast | Fast |
| LICs | Fast | Central | Slow | Fast | Fast |

HICs, MICs, and LICs stand for high-, middle-, and low-income countries, respectively

**Table 4** Land-use conversion difficulty levels in the Greater Bay Area under each SSP

| Land-use conversion | SSP1 | SSP2 | SSP3 | SSP4 | SSP5 | Reference policy |
|---|---|---|---|---|---|---|
| Transition from cropland to urban area | Moderate | Moderate | Easy | Easy | Easy | The cultivated land requisition–compensation balance policy[a,b,c] |
| Transition from cropland to others | Difficult | Moderate | Easy | Moderate | Moderate | Implement the strictest cropland protection system[b,c] |
| The increase in well-facilitated farmland | Easy | Moderate | Difficult | Difficult | Easy | Promote the development of well-facilitated farmland[b,c] |
| Transition from forest to cropland | Easy | Moderate | Easy | Easy | Easy | The cultivated land requisition–compensation balance policy[a,b,c] |
| Transition from forest to others | Difficult | Moderate | Easy | Moderate | Moderate | Restore forest ecosystem[b,c] |
| The increase in forest | Easy | Moderate | Difficult | Difficult | Moderate | Expand forest cover[b,c] |
| The increase in urban built-up land | Moderate | Moderate | Easy | Moderate | Moderate | Improve the urbanization rate while strictly controlling the approval of new built-up land[b,c] |
| The increase in rural built-up land | Difficult | Moderate | Easy | Difficult | Difficult | Revitalize the existing rural built-up land; the abandoned houses and hollow villages in rural areas will be demolished and reclaimed into new built-up land for urban development[b,c] |
| Transition from barren land to built-up land | Easy | Moderate | Difficult | Easy | Easy | |
| Transition from water to others | Difficult | Moderate | Easy | Moderate | Moderate | Strictly protect the water ecological space along the shoreline of the water area and prohibit the reclamation of lakes or encroachment on river courses[b,c] |

The superscripts [a], [b], and [c] indicate that the policy was derived from Letter of support for the Guangdong–Hong Kong–Macao Greater Bay Area and Shenzhen to explore the reform of natural resources, Land Planning of Guangdong Province (2016–2030), and Land Planning of Guangdong Province (2016–2035), respectively

**Table 5** Conversion cost matrix of SSP2

| Land-use classes | Cropland | Bush and grassland | Forest | Water | Urban area | Barren land |
|---|---|---|---|---|---|---|
| Cropland | 0.000 | 0.100 | 0.900 | 0.800 | 0.100 | 0.400 |
| Bush and grassland | 0.500 | 0.000 | 0.800 | 0.400 | 0.300 | 0.100 |
| Forest | 0.700 | 0.300 | 0.000 | 0.990 | 0.990 | 0.800 |
| Water | 0.900 | 0.900 | 0.900 | 0.000 | 0.990 | 0.500 |
| Urban area | 1.000 | 1.000 | 1.000 | 1.000 | 0.000 | 1.000 |
| Barren land | 0.900 | 0.500 | 0.990 | 0.800 | 0.300 | 0.000 |

The table was derived from Table 1 provided by Liu et al. (2017)

natural resources (People's government of Guangdong province 2020) were used as the references. The future land-use policies relevant to the period around 2030 were then extracted and taken as a reference for SSP1 as the sustainable development of the Guangdong province was integrated into a strategic goal (People's government of Guangdong province 2019). The difficulty of combining land-use narratives (Popp et al. 2017) (Table 3) with the local land planning policy under each SSP can be at one of three levels: difficult, moderate, and easy (Table 4). In the second step, SSP2 was considered to be the basic reference, and the conversion cost matrix derived from Liu et al. (2017) was assumed to be the SSP2 conversion cost matrix (Table 5) as it was estimated based on the opinions of local experts and the analysis of

historical land use. Next, 1.5, 1.0, and 0.5 were identified as the difficult, moderate, and easy levels, respectively, using test methods. Considering the qualitative difficulty level of land-use conversion in each SSP (Table 4) and the values of the three difficulty levels used to adjust the SSP2 conversion cost matrix, the conversion cost matrices for SSP1, SSP3, SSP4, and SSP5 were obtained (Tables S1–S4).

Finally, after defining the future land demands and conversion cost matrix for each SSP, the linear programming (LP) method was used to determine the land transition probability matrices for each SSP (Table S5–S9) using the solver function of Microsoft Excel (Plus 2019 version). The LP approach for determining the land transition probability is a relatively new method employed in scenario analysis

(DasGupta et al. 2019). The derivation of the land transition probability matrix $M$ ($= [m_{ij}]$), where the $m_{ij}$ values denote the land transition probability from land-use class $i$ to $j$ for a given period, was proposed by Hashimoto et al. (2019).

Based on all the processes described above, the land-use maps of the Greater Bay Area under the different SSPs could be projected for 2030 using the LCM.

The land-use narrative was derived from the work by Popp et al. (2017). The narratives of population growth and urbanization level were derived from the work by Jones and O'Neill (2016). The demographic factors driving population change in countries were categorized into the following groups as a function of the fertility and income levels: high fertility, low fertility with high income (i.e., as in the member countries of the Organization for Economic Cooperation and Development), and low fertility. The population projections of the Greater Bay Area in 2030 under SSPs were derived from the work by Chen et al. (2020b), and their spatial distribution maps were used to shape the future land-use patterns in LCM, please see the section "Step 4: Planning constraints and incentives" for details.

## Biocapacity calculations under various SSPs

Biocapacity (BC) expresses the supply of resources and ecological services, whereas the ecological footprint (EF) is a measure of the human demand for resources and ecological services (Wackernagel and Rees 1996). BC and EF could be used as indicators for the examination of the possibility of achieving sustainable development (Moran et al. 2008). In this study, the BC values for the six land-use classes were calculated based on the land-use maps projected for 2030 under each SSP. The values were compared with the BC and EF values of 2015 to estimate the extent of the sustainable trend. The BC value was calculated using the following equation (see Borucke et al. (2013) for the methodological details):

$$BC = \sum_i \frac{A_i}{N} \cdot YF_i \cdot EQF_i, \qquad (1)$$

where $BC$ (gha/cap) is the per capita biocapacity; $A_i$ (ha), the area available for the land-use class $i$; $N$, the population; and $YF_i$ (wha/ha) and $EQF_i$ (gha/wha), the yield factors and equivalence factors of the land-use class $i$, respectively (Table 6). The units "gha" and "wha" stand for global hectare and world average hectare, respectively [see Global footprint network (2020a) and the Working Guidebook to the National Footprint and Biocapacity Accounts (NFAs) (Global footprint network 2019) for more details.]

The yield factors were derived from the study by Liu et al. (2010) and the other equivalence factors from the NFA (Global footprint network 2019). The original equivalence factors of grassland and bush were 0.46 and 1.29, respectively, and the corresponding yield factors were 2.71 and 1.03, respectively. As grassland and bush were grouped into one land-use class in this study, they were represented by average values.

## Carbon emissions coming from land use

Being a typical human activity, land use has influenced the global carbon balance by changing the natural carbon sources and sinks, such as forest, grassland, and cropland (Caspersen et al. 2000; Houghton et al. 2012). However, with the increased industrialization and urbanization, changes in the land-use patterns are causing increased carbon emissions (Zhang et al. 2018). Therefore, the carbon emission trend associated with land use under each SSP was estimated (Yang et al. 2020; Cao and Yuan 2019) using the following equation:

$$E_s = \sum_i A_{si} \cdot \delta_i, \qquad (2)$$

where $E_s$ (tC.y$^{-1}$) denotes carbon emissions occurring under Scenario $s$; $A_{si}$ (ha), the area of land-use class $i$ under

**Table 6** Equivalence and yield factors of different land-use classes

| Land-use classes | Cropland | Forest | Bush and grassland | Water | Urban area | Barren land |
|---|---|---|---|---|---|---|
| Equivalence factors | 2.52 | 1.29 | 0.88 | 0.37 | 2.52 | 2.52 |
| Yield factors | 1.65 | 1.03 | 1.87 | 2.71 | 1.74 | 1.74 |

**Table 7** Carbon emission coefficient [in tC/(ha y$^{-1}$)] of each land-use class

| Land-use class | Cropland | Forest | Bush and grassland | Urban area | Barren land | Water |
|---|---|---|---|---|---|---|
| Value | 0.422 | − 0.644 | − 0.021 | 40.73 | − 0.005 | − 0.253 |
| Reference | (Yang et al. 2019) | (Yang et al. 2019) | (Shi et al. 2012) | (Shi et al. 2012) | (Shi et al. 2012) | (Shi et al. 2012) |

**Table 8** Past land-use changes (km²) and their percentages (given within parenthesis) in the Greater Bay Area from 2000 to 2010

| Land-use class | 2000 | | 2010 | | Gain | Loss | Net change |
|---|---|---|---|---|---|---|---|
| Cropland | 22,603 | (40.54) | 20,839 | (37.37) | 336 | − 2,100 | − 1,764 |
| Forest | 23,283 | (41.76) | 23,096 | (41.42) | 508 | − 696 | − 188 |
| Bush and grassland | 3,191 | (5.72) | 2,261 | (4.06) | 408 | − 1,337 | − 929 |
| Urban area | 2,886 | (5.18) | 5,904 | (10.59) | 3,018 | 0 | 3,018 |
| Barren land | 6 | (0.01) | 3 | (0.01) | 0 | − 3 | − 3 |
| Water | 3,789 | (6.80) | 3,655 | (6.56) | 25 | − 158 | − 133 |
| Total | 55,758 | | 55,758 | | | | |

Scenario $s$; and $\delta_i$, the carbon emission (absorption) coefficient (tC/(ha y⁻¹)) of a given land-use class $i$. The carbon emission (absorption) coefficients are shown in Table 7.

## Results

### Historical land-use changes and transition modeling

From Table 8, it can be seen that all land-use classes except urban area experienced both a gain and a loss; urban area recorded only an increase in the land area (3,018 km²). The contributors to the net increase in the urban area, in the descending order of their contributions, are cropland (2000 km²), bush and grassland (847 km²), forest (95 km²), water (73 km²), and barren land (3 km²).

In the study, 26 transitions (covering 99% of the total transitions) and persistence were grouped into five submodels (Table S10). The MLPNN method demonstrated good performance. All of the accuracy rates of the submodels were higher than 0.800. Moreover, all the transitions showed a high skill measure with the lowest at 0.631 (transition from water to bush and grassland) and

the highest at 1.000 (transition from forest to cropland and cropland to forest).

Using historical changes and transition potential submodels, the LCM could determine how the 12 variables (Fig. 4) influenced future changes and the magnitude of those changes. The extent of land-use transitions in 2030 was then calculated for the BaU scenario. Based on BaU scenario model, land-use projections for different SSPs were generated by adjusting the land transition probability matrix as shown in Fig. 3 and as described in the section "Correlating land-use modeling with the local land planning policy-coupled SSPs".

### Assessment of predictive performance of the model

The projected land-use map of 2015 and the actual land-use map of 2015 were used to calculate the confusion matrix (Table 9). The overall accuracy and Kappa coefficient (Mohammady et al. 2015) were 0.96 and 0.93, respectively. Precision and recall are two important model evaluation metrics (Saxena 2018). Precision is the fraction of the images that project a particular land-use class that turns out to actually have that land-use class; recall is the fraction of images with a particular land-use class that have been projected to have that land-use class (Leung and Newsam

**Table 9** Validation of predictive performance of the model

| | Land-use classes | Projected land-use map in 2015 | | | | | | | Recall |
|---|---|---|---|---|---|---|---|---|---|
| | | Cropland | Bush and grassland | Forest | Water | Urban area | Barren land | Area (km²) | |
| Actual land-use map in 2015 | Cropland | 19,526 | 8 | 93 | 2 | 876 | 0 | 20,506 | 0.95 |
| | Bush and grassland | 36 | 1,627 | 283 | 6 | 312 | 0 | 2,264 | 0.72 |
| | Forest | 147 | 243 | 22,563 | 10 | 16 | 0 | 22,979 | 0.98 |
| | Water | 15 | 28 | 7 | 3,520 | 30 | 0 | 3,600 | 0.98 |
| | Urban area | 285 | 20 | 15 | 48 | 6,037 | 1 | 6,406 | 0.94 |
| | Barren land | 0 | 0 | 0 | 0 | 0 | 1 | 1 | 1.00 |
| | Area (km²) | 20,008 | 1,927 | 22,962 | 3,586 | 7,271 | 3 | 55,758 | |
| Precision | | 0.98 | 0.84 | 0.98 | 0.98 | 0.83 | 0.53 | | Overall accuracy: 0.96 |
| F score | | 0.96 | 0.78 | 0.98 | 0.98 | 0.88 | 0.70 | | Kappa: 0.93 |

Decimal figures of area were converted to the nearest integers
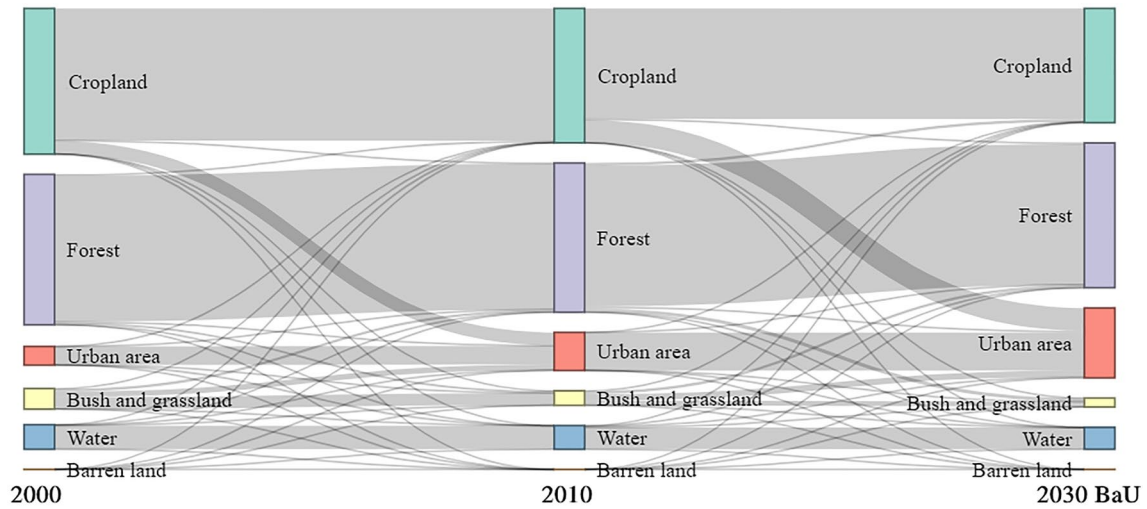
**Fig. 5** Land-use change flow in the Greater Bay Area for three time slices: 2000, 2010, and 2030 BaU map

2012). Furthermore, the *F* score enables the combination of the precision and recall metrics into a single measure that captures both properties (Brownlee 2020), it is calculated as (2 × Precision × Recall)/(Precision + Recall). The *F* scores of cropland (0.96), forest (0.98), urban area (0.88), and water (0.96), which constitute the largest proportion of

the land area in the Greater Bay Area, were very high. By contrast, the *F* score of bush and grassland (0.78) and barren land (0.70) were relatively low. However, these two land-use classes do not significantly affect the predictive accuracy as their contributions to it are small. Therefore, the validation
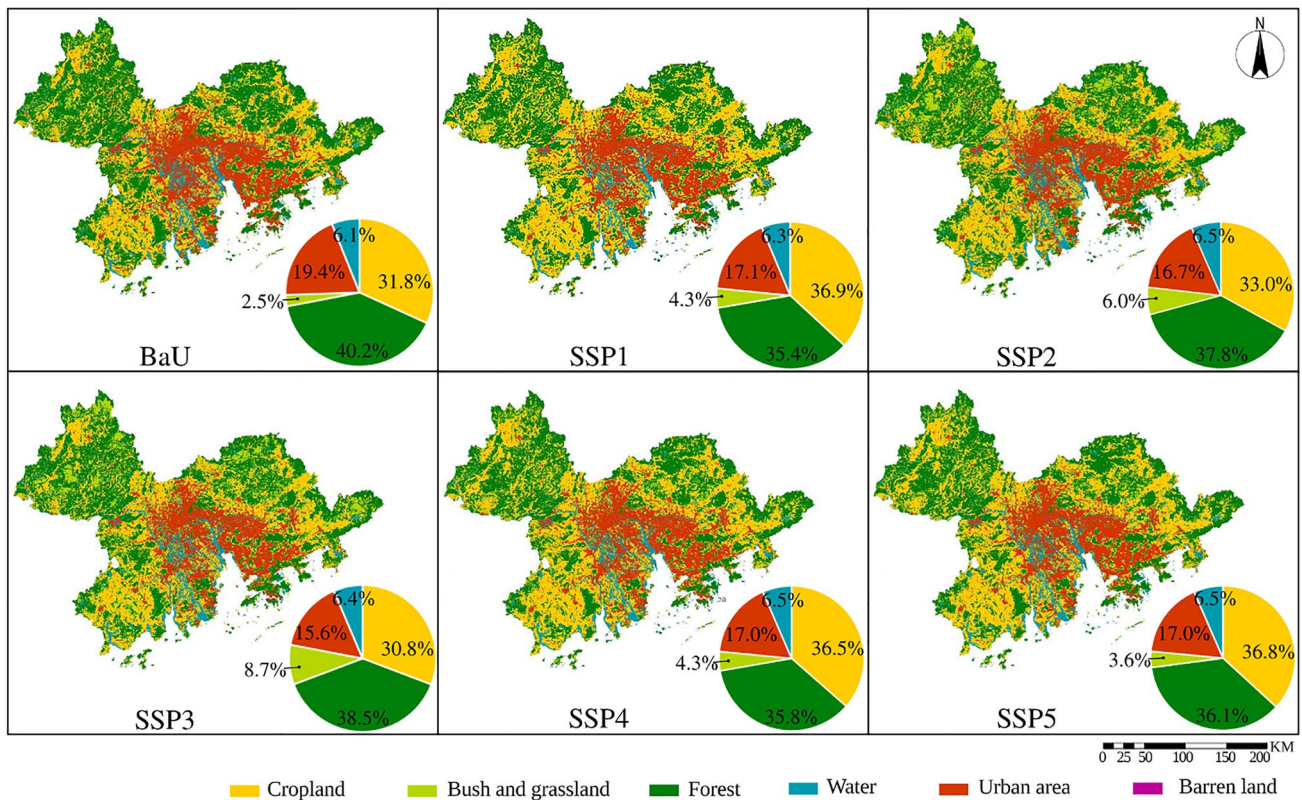


**Fig. 6** Projected land-use maps of the Greater Bay Area in 2030 under various SSPs at a 300-m resolution

demonstrated that the proposed model has a high predictive ability.

## Future land-use changes under different scenarios

The historical trends of land-use changes in the Greater Bay Area (Fig. 5) from 2000 to 2030 demonstrate that, in general, the dominant land-use classes were cropland, forest, and urban area. Moreover, the proportion of land classified as urban area continuously and significantly increased; cropland, bush, and grassland experienced a significant decline, and forest exhibited a relatively small decrease. The conversion of cropland into urban area was a major contributor to urban development; approximately 22% of cropland had been converted into urban area between 2000 and 2030.

The spatial land-use distribution pattern of each scenario has not significantly changed (Fig. 6); thus, urban development still revolves around Pearl River Delta, which is surrounded by cropland, with forest predominantly located on its north side. The proportions of cropland, forest, and urban area are the highest. In the BaU scenario, which assumes the continuation of past trends without any constraints or incentives, the proportions of urban area (19.4%) and forest (40.2%) are larger than those under the SSP scenarios

(Table 10; Fig. 7), whereas the proportion of bush and grassland (2.5%) is relatively low. In the SSPs, cropland and urban area were the largest in SSP1, being 1.16 and 0.88 times the size of BaU, respectively, followed by their respective areas in SSP5 and SSP4. Contrarily, the forest area in SSP1 (19,747 km$^2$) was relatively low. In SSP3, the urban area (8,703 km$^2$; 0.80 times the size of BaU) and cropland (17,159 km$^2$; 0.97 times the size of BaU) were the lowest. Significantly, only in SSP3, cropland was smaller than that in BaU.
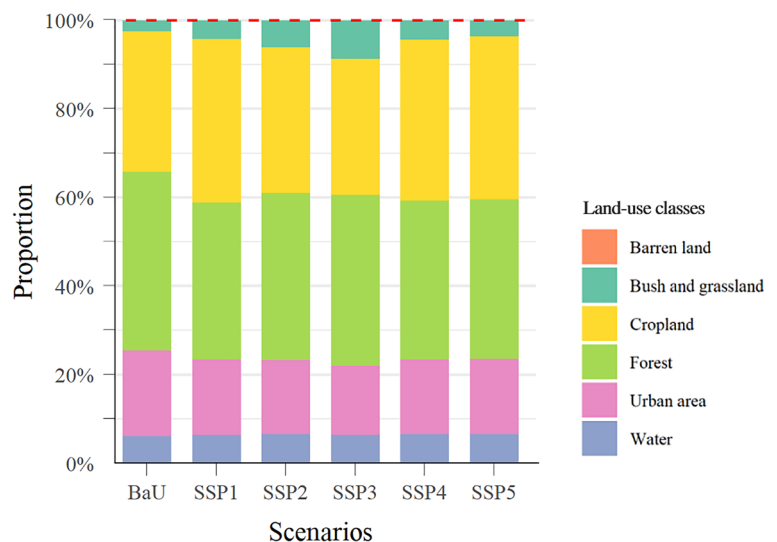
## Assessment of Hong Kong under various SSPs

The projected land-use maps of Hong Kong were extracted from those of Greater Bay Area using ArcGIS pro (the projected land-use maps can be obtained for other metropolitan regions, such as Shenzhen, Guangzhou, and Macao). As shown in Fig. 8, Hong Kong has five land-use classes. Although the areas of the different land-use classes depend on the scenario considered, the land-use spatial distributions under different SSPs are similar. The forest, and bush and grassland areas under SSP1, SSP2, SSP4, and SSP5 are less than the respective areas under SSP3. The urban area under SSP3 has become small and the cropland area has shrunk

**Table 10** Land-use areas of the Greater Bay Area in 2030 under different SSPs and BaU (in km$^2$). The figure given within the brackets denotes the proportion with respect to that observed under the BaU assumption

| Scenarios | Cropland | | Forest | | Bush and grassland | | Urban area | | Barren land | | Water | |
|---|---|---|---|---|---|---|---|---|---|---|---|---|
| BaU | 17,728 | | 22,414 | | 1,396 | | 10,829 | | 3 | | 3,388 | |
| SSP1 | 20,568 | (1.16) | 19,747 | (0.88) | 2,372 | (1.70) | 9,557 | (0.88) | 3 | (1.00) | 3,511 | (1.04) |
| SSP2 | 18,386 | (1.04) | 21,080 | (0.95) | 3,354 | (2.40) | 9,325 | (0.86) | 3 | (1.00) | 3,610 | (1.07) |
| SSP3 | 17,159 | (0.97) | 21,463 | (0.96) | 4,871 | (3.49) | 8,703 | (0.80) | 3 | (1.00) | 3,559 | (1.05) |
| SSP4 | 20,336 | (1.15) | 19,959 | (0.89) | 2,386 | (1.71) | 9,468 | (0.87) | 3 | (1.00) | 3,606 | (1.06) |
| SSP5 | 20,538 | (1.16) | 20,112 | (0.90) | 2,006 | (1.44) | 9,468 | (0.87) | 3 | (1.00) | 3,631 | (1.07) |

**Fig. 7** Proportion of each land-use class of the Greater Bay Area under various SSPs and BaU assumption
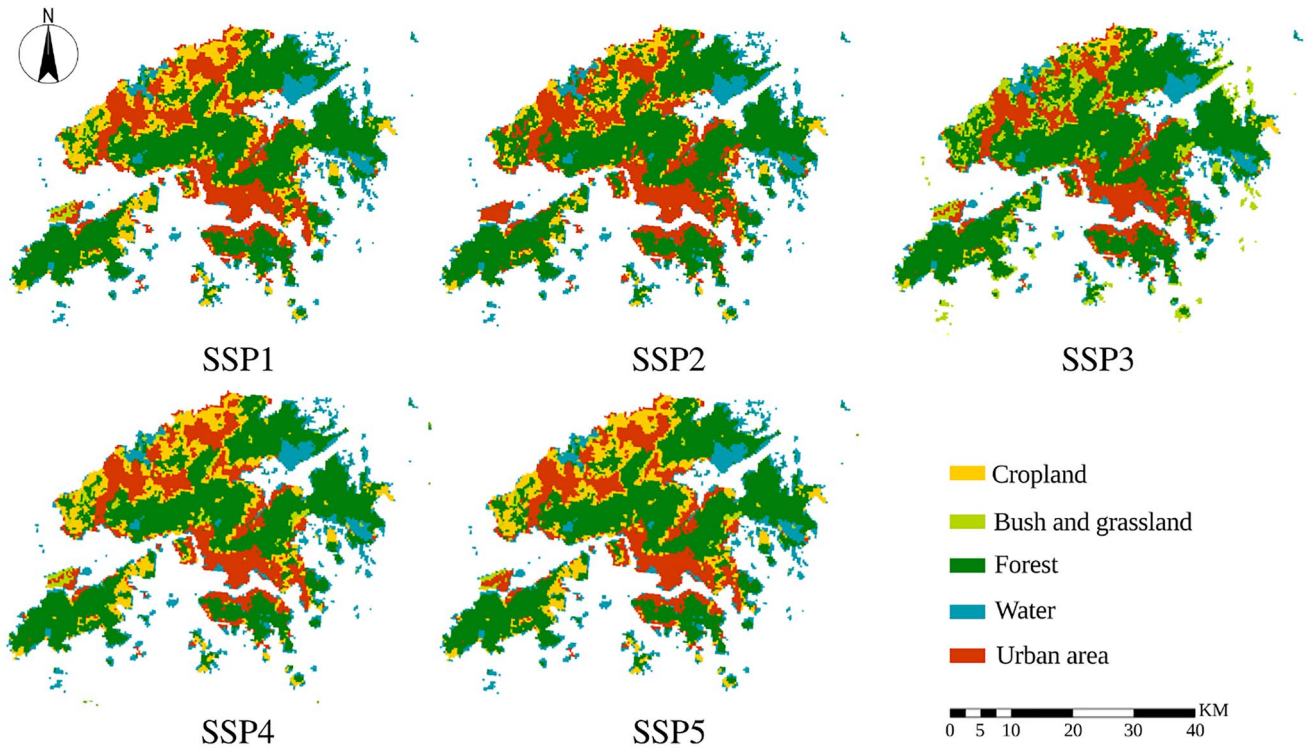
**Fig. 8** Projected land-use maps of Hong Kong in 2030 under various SSPs

**Fig. 9** A comparison of the per capita ecological footprint (EF) of China and Hong Kong in 2015 and 2030 and a comparison of the per capita biocapacities of China and Hong Kong in 2015 and 2030 under each SSP. (The bar chart and dashed lines denote the biocapacity and EF in gha/cap, respectively. The data pertaining to the biocapacity and EF of Hong Kong in 2015 were obtained from the study by Shi et al. (2020). The data pertaining to the EF of China in 2015 were derived from the Global footprint network (2020b))
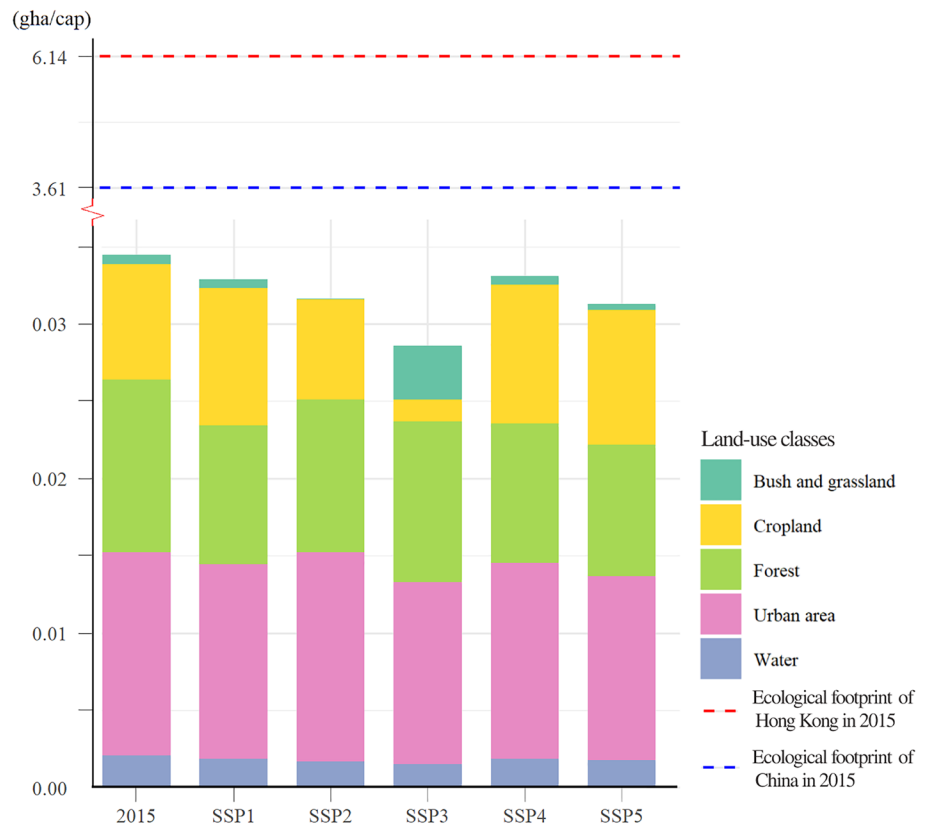
**Table 11** Per capita biocapacity of Hong Kong in 2015 and 2030 under each SSP (gha/cap)

| | Cropland | Forest | Bush and grassland | Urban area | Water | Total |
|---|---|---|---|---|---|---|
| SSP1 | 0.00903 | 0.00895 | 0.00054 | 0.01313 | 0.00171 | 0.0334 |
| SSP2 | 0.00650 | 0.00989 | 0.00003 | 0.01350 | 0.00171 | 0.0316 |
| SSP3 | 0.00140 | 0.01039 | 0.00351 | 0.01176 | 0.00154 | 0.0286 |
| SSP4 | 0.00898 | 0.00903 | 0.00054 | 0.01265 | 0.00188 | 0.0331 |
| SSP5 | 0.00871 | 0.00849 | 0.00039 | 0.01192 | 0.00177 | 0.0313 |
| 2015 | 0.00749 | 0.01117 | 0.00059 | 0.01313 | 0.00208 | 0.0345 |

significantly. These results agree with SSPs narratives; because of limited land-use regulation the lowest urbanization level occurs under SSP3 (Table 3), and the transition from cropland to other land-use classes is easy, whereas increasing well-facilitated farmland is difficult under SSP3 (Table 4). Under the other SSPs, the urbanization level is central or fast, land-use regulation is medium or strong, and the growth of land productivity is high (Table 3).

### Future biocapacity of Hong Kong under each SSP scenario

As can be seen from Fig. 9, the biocapacities of urban area, forest, and cropland are the dominating categories. As Table 11 shows, the per capita biocapacity in 2030 under each of the SSPs has declined from its value in 2015 (0.0345 gha/cap). In 2015, it has the highest value under SSP1 (0.0334 gha/cap) and the lowest value under SSP3 (0.0286 gha/cap). During the period from 2015 to 2030, the per capita biocapacities of cropland under SSP1, SSP4, and SSP5 have improved but decreased under SSP2 and SSP3. However, the per capita biocapacity of urban area has increased (0.01350 gha/cap) only under SSP2, whereas under each of the other SSPs, its value is less than or equal to its value in 2015 (0.01313 gha/cap). The per capita biocapacities of forests have reduced in 2030 in all SSPs.

Between the per capita EF of Hong Kong in 2015 (6.14 gha/cap) and that in 2030 under SSP1, which is the highest among all the SSPs, a significant gap exists (Fig. 9). The per capita ecological footprint of Hong Kong is around 184 times the per capita biocapacity; this indicates that the demands made by the population far exceed the supplies of the local ecosystem. In addition, being a developed city, the per capita consumption in Hong Kong is approximately 1.7 times the per capita consumption of China (3.61 gha/cap).

### Future carbon emissions from land-use in Hong Kong

From Table 12 and Fig. 10, it can be seen that urban area (366.57 tC/ha) and cropland (3.80 tC/ha) are the main contributors to the emissions. The urban area has a decisive impact on the carbon emission increase in Hong Kong. Contrarily, forest (− 5.80 tC/ha), bush and grassland (− 0.19 tC/ha), and water (− 2.27 tC/ha) contributed to the absorption of carbon; forests in particular play a major role in absorbing carbon. The $CO_2$ emissions from land use in 2030 were approximately 8% of the total emissions in 2015. The highest $CO_2$ emission was under SSP2, which was caused by the large emissions that came from the urban area (3,797,700 $tCO_2.y^{-1}$); it was followed by the emissions under SSP1, SSP5, and SSP4. The emission from cropland in SSP5 (27,900 $tCO_2.y^{-1}$) was the largest, whereas the emission from cropland in SSP3 (4,000 $tCO_2.y^{-1}$) was the smallest. The $CO_2$ absorption from forests were the first and second largest under SSP2 and SSP3 (− 145,300 $tCO_2$.

**Table 12** Carbon emissions/absorptions ($10^2$ tC.y$^{-1}$) from different land-use classes in Hong Kong in 2030 under each SSP. The figure in brackets denotes the value converted to $CO_2$ ($10^2$ $tCO_2.y^{-1}$)

| | Total | | Cropland | | Forest | | Bush and grassland | | Urban area | | Water | |
|---|---|---|---|---|---|---|---|---|---|---|---|---|
| SSP1 | 9,666 | (35,474) | 75 | (275) | − 355 | (− 1,303) | − 0.56 | (− 2.06) | 9,982 | (36,634) | − 35 | (− 128) |
| SSP2 | 9,971 | (36,594) | 54 | (198) | − 396 | (− 1,453) | − 0.03 | (− 0.11) | 10,348 | (37,977) | − 36 | (− 132) |
| SSP3 | 8,167 | (29,973) | 11 | (40) | − 396 | (− 1,453) | − 3.52 | (− 12.92) | 8,585 | (31,507) | − 30 | (− 110) |
| SSP4 | 9,218 | (33,830) | 74 | (272) | − 355 | (− 1,303) | − 0.56 | (− 2.06) | 9,538 | (35,004) | − 38 | (− 139) |
| SSP5 | 9,239 | (33,907) | 76 | (279) | − 355 | (− 1,303) | − 0.43 | (− 1.58) | 9,556 | (35,071) | − 38 | (− 139) |
| Total $CO_2$ emissions in 2015 | 416,000 | | | | | | | | | | | |

The total $CO_2$ emissions in 2015 were derived from The Environmental Protection Department of Hong Kong (2017). The emissions include those due to land use, electricity generation, town gas production, transport, industrial processes, product use, and the other end uses of fuel
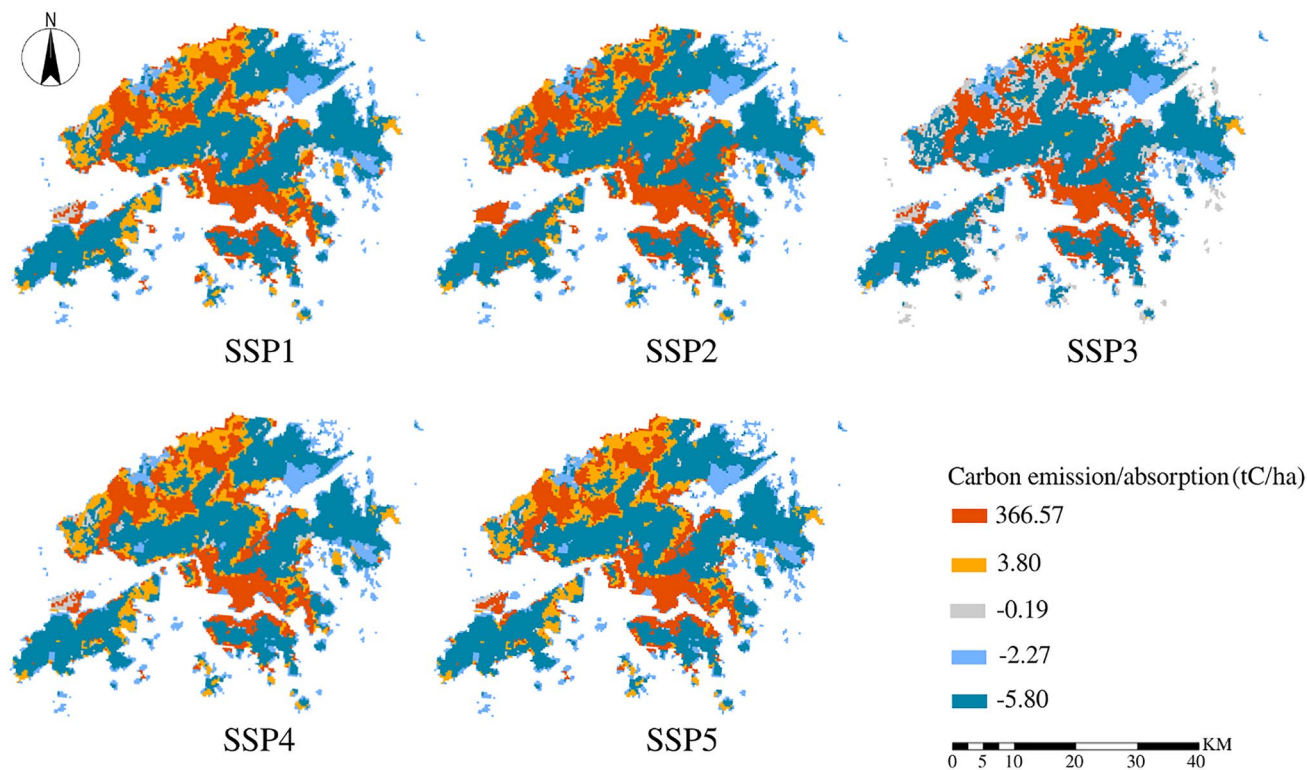
The values were converted to their nearest integers

**Fig. 10** Spatial distributions of the carbon emissions (absorptions) in Hong Kong in 2030 under each SSP

y$^{-1}$), respectively, whereas its values under SSP1, SSP4, and SSP5 were almost same.

## Discussion

### Advantages and limitations of the study

The studies by Hasan et al. (2020), Jiao et al. (2019), and Song et al. (2020) were similar to the present study with respect to the model, study area, and scenarios, respectively. Therefore, the scenarios, LULC models, and advantages and disadvantages of the methods used by the three previous studies mentioned and our study were compared (Table S11) to demonstrate the differences of the four studies.

As can be seen from Table S11, the present study has two prominent advantages over the other three studies, which are listed as follows:

(1) Spatial downscaling framework: this framework can also be used for other regions in China, such as Yangtze River Delta and Beijing–Tianjin–Hebei Urban Agglomeration, or other scenarios to simulate the future land-use patterns. The output map with a high resolution could help understand the implications of global environmental changes and greenhouse gas (GHG), which are crucial for studying sustainable development (Solecki and Oliveri 2004).

Among the various land-use classes, the urban and agricultural land use are the two most commonly recognized high-level classes of land use (Zhu et al. 2019). A map with an improved resolution can provide detailed and accurate land-use information for urban planning, environmental monitoring, and governmental management (Rawat and Kumar 2015). For instance, a 300-m resolution map can be used to observe the impact of urbanization on the land system in terms of space and time (Liu et al. 2020; van Vliet 2019), thereby helping decision-makers and stakeholders to design and coordinate sustainable urban development plans (Chapa et al. 2019).

(2) Elaboration of qualitative and quantitative methods of correlating LCM with localized SSPs: this is the most challenging part of scenario-based land-use modeling and could make a significant impact on the projected results. However, the three previous studies did not make this elaboration. The qualitative and quantitative methods proposed in this study could be improved by considering additional factors, such as demographic, environmental, and economic factors, that would facilitate a more comprehensive and integrated simulation method for land-use change projection.

The study also had several limitations. Future infrastructure development, such as the construction of new roads, was not included in the future projections made in the study, which can affect the spatial patterns of urban expansion and

associated land-use changes under the different scenarios. Besides, the yield factor and equivalence factor of the biocapacity would vary, depending on the level of technology and socioeconomic development of the SSP considered. For instance, owing to the improvements in agricultural productivity (Table 3), the yield factor can be relatively high in SSP1 and SSP5 and could thus lead to a large local biocapacity. However, due to data limitations, the biocapacity was calculated for each scenario using the same set of yield factors (2001) and equivalence factors (2019). In the section "Correlating land-use modeling with the local land planning policy-coupled SSPs", we referred to Liao et al. (2020), Li and Chen (2020), and Li et al. (2016) in adjusting future land demands because reference data for all land-use classes could not be obtained from a single source. To maintain data consistency, all references were selected in accordance with SSPs narratives. The Chinese research community can establish a unified and localized SSPs database for simulating and applying future projections. Although GHG includes $CO_2$, $CH_4$, $N_2O$, and fluorinated gases (Ritchie and Roser 2017; United States Environmental Protection Agency 2018), in this study, only $CO_2$ emissions were considered and estimated only in terms of the land-use factor. Other emission factors, including economic development, population, energy consumption, and production, also require consideration.

## Verification and validation

As shown in Table 3, from among the different socioeconomic development pathways possible in the future, urbanization will rapidly proceed under SSP1 and SSP5, whereas population growth will become relatively low with good land-use regulation and agricultural productivity improvements. Under SSP4, the urbanization level is relatively fast, and only high- and middle-income countries or upper/middle classes would be able to regulate land use and stimulate productivity. Under SSP2, land-use regulation, productivity, and population growth are all at a medium level with concentrated urbanization. However, SSP3 represents the worst-case scenario, where population growth stands in stark contrast with slow urbanization, low land-use regulation, and low productivity.

The results obtained for biocapacity (Fig. 9; Table 11) are compatible with the SSPs narratives previously mentioned. The gaps among the biocapacities under different SSPs are mainly due to the variations in their cropland and urban areas. The urban area growth in SSP3 is lower than that in either SSP1 or SSP5, due to the differences in the human development trends caused by factors such as population and GDP growth (Li et al. 2019; Hausfather 2018; He et al. 2017). In addition, due to the pressure exerted by population growth and rapid rate of urbanization, China has

implemented strict cropland protection and balance policies to ensure food security (Li and Chen 2020). Therefore, in the Greater Bay Area, the two largest cropland areas that support the sustainable development of the human society are under SSP1 and SSP5, followed by the cropland areas under SSP4 and SSP2.

However, what is good for the sustainable development of human society need not necessarily be good for the nature. The rapid development of the urban area and the implementation of cropland balance policies could be disadvantageous for low-carbon development. As presented in Table 12, the carbon emissions from land use under SSP2, SSP1, and SSP5 are the highest. According to the analysis of historical land-use transitions (Fig. 5), cropland is the main land class that can meet the requirements of urban expansion. However, in the future, the cost of urban sprawl will be indirectly transferred from cropland to other land classes, such as by the shrinking of forest, and bush and grassland, leading to a relatively low demand for forest in SSP1 (Table 2) due to the implementation of strict cropland protection and cultivated land requisition–compensation balance policy under SSP1 (Table 4). The loss of vegetation would also lead to a decline in carbon absorptions and thus will not be conducive for achieving carbon neutrality before 2060 (Mallapaty 2020).

## Policy implications

As indicated below, the implications of future sustainable development can be explored by considering the future land-use projections made by this study.

### Biocapacity optimization

As shown in Eq. (1) and Table 6, biocapacity is determined mainly by two factors: land area and land productivity (WWF 2019). The biocapacity would enhance if the two key drivers could be improved. Our results demonstrate that the areas of different land-use classes would vary depending on the scenario (Figs. 6 and 8), and that with limited land-use change regulation (SSP3), both the local biocapacity and cropland biocapacity would decline significantly (Fig. 9). By contrast, the strict control of land-use conversions would mitigate the degradation of local biocapacity (SSP1 and SSP4); the local biocapacity of cropland under SSP1 is high because of improved agricultural productivity (Table 3). Nevertheless, the level of agricultural industrialization in the Greater Bay Area is still low, with backward agricultural socialization service systems and an imbalance in the development of different cities (Wan and Han 2019; ScienceNet.cn 2019; Gu 2019). Therefore, according to the results of our analysis, the biocapacity in the Greater Bay Area can be significantly improved by enhancing the

productivity of agriculture and the regulation of land-use conversions.

## Mitigation of $CO_2$ emissions

Urban area and cropland are the main sources of emissions (Fig. 10), whereas vegetation-covered areas and water are the main contributors to carbon absorptions. Thus, the three highest $CO_2$ emissions from land use occur under SSP2, SSP1, and SSP5 because the urban and cropland areas under these three scenarios are the largest of the corresponding areas under the five scenarios. Under SSP3, the emissions are low because the urban area and cropland under the scenario are small with large vegetation-covered areas. Thus, the green and blue spaces are important and effective in mitigating $CO_2$ emissions. However, according to Tables 8 and 10, the green and blue spaces have been declining since 2000. The trend would continue into the future. To mitigate $CO_2$ emissions and achieve carbon neutrality before 2060, more attention would be required to the construction of blue-green infrastructure while building cities in the Greater Bay Area.

## Further improvements

The cultivated land requisition–compensation balance policy was released in 1997 (The National People's Congress of the PRC 2019). Although it has been upgraded from a quantity- and quality-oriented policy to an ecological balance-oriented policy (Han et al. 2018), various issues, such as inequities in crossregional transitions and imbalance of cultivated land quality, continue to appear. A large proportion of reclaimed cultivated land, which was not suitable for paddy cultivation, has been provided in mountainous areas to compensate for the loss of paddy land in the plains (Chen et al. 2019a; Tang et al. 2020; Gu et al. 2019). Moreover, when we considered this policy in our future land-use projections for the Greater Bay Area (Table 4), we found that it was beneficial mainly for developing urban area and protecting cropland rather than maintaining a balance among all land-use classes. For instance, the cost of urban sprawl is indirectly transferred from cropland to forest, and bush and grassland (as shown in the section "Verification and validation"). In this way, not only the biocapacity of cropland could would not be maintained but also the capacity of carbon absorption would decrease, which would be detrimental to both socio-economic and environmentally sustainable development. Therefore, the current ecological balance mechanism and regulatory regime require further improvement by considering urban area and cropland, and the balance among all land-use classes.

## Future prospects

Currently, scenarios about socioeconomic future prospects, such as the SSPs, are playing a major role in making projections (Nilsson et al. 2017). However, these scenarios have limitations in their applicability to biodiversity and nature research (Pereira et al. 2020; Rosa et al. 2017). To fill the gap, nature-centered scenarios, including the Nature Futures Framework (NFF), developed by the Intergovernmental Science-Policy Platform on Biodiversity and Ecosystem Services (IPBES), were proposed. The NFF describes positive relationships between people and nature, from multiple aspects, such as nature as culture, nature for society, and nature for nature (Lundquist et al. 2020), to capture interlinkages of social-ecological systems across biodiversity, ecosystem functions and services, and human well-being (IPBES 2016b; Rosa et al. 2020). In Japan, a new research project named Predicting and Assessing Natural Capital and Ecosystem Services (PANCES), which uses an integrated social-ecological system approach, was launched to predict and assess the natural capital and ecosystem services under national-scale future scenarios (Saito et al. 2019). A strong international cooperation is also being established. The IPBES-IPCC co-sponsored workshop, which was the first collaboration between IPBES and IPCC, was held in December 2020 to build a multidisciplinary expert group to meet both climate change- and biodiversity-related goals (IPBES 2020). Therefore, the combination of socioeconomic scenarios and nature-centered scenarios will become more productive toward the sustainable development of cities in the future.

## Conclusion

This study aimed to project future land-use patterns at a relatively high resolution to explore SSPs implications and the possible land-use changes due to urban development. Through a spatial downscaling framework that combines global SSPs narratives with local land planning policies, using a land change modeling method, the study revealed that all of the scenarios experienced a significant expansion of urban area at varying degrees of decrease in cropland and forest, thereby leading to considerable differences in the levels of local biocapacity and carbon emissions. The effects of intervention policies, such as the local land planning policy and cultivated land requisition–compensation balance policy, were examined, and our analysis revealed that they were beneficial mainly for developing urban area and protecting cropland rather than maintaining a balance among all land-use classes. Our findings would

contribute to the improvement of intervention policies related to the research area.

# References

Acheampong M, Yu Q, Enomah LD, Anchang J, Eduful M (2018) Land use/cover change in Ghana's oil city: assessing the impact of neoliberal economic policies and implications for sustainable development goal number one—a remote sensing and GIS approach. Land Use Policy 73:373–384

Allen C, Metternicht G, Wiedmann T (2017) An iterative framework for national scenario modelling for the Sustainable Development Goals (SDGs). Sustain Dev 25(5):372–385

Asia N (2020) Hong Kong wants a massive new island, but where will it get the sand? https://asia.nikkei.com/Opinion/Hong-Kong-wants-a-massive-new-island-but-where-will-it-get-the-sand. Accessed 9 December 2020

Aung TS, Fischer TB, Buchanan J (2020) Land use and land cover changes along the China-Myanmar Oil and Gas pipelines–Monitoring infrastructure development in remote conflict-prone regions. PLoS ONE 15(8):e027806

Borucke M, Moore D, Cranston G, Gracey K, Iha K, Larson J, Lazarus E, Morales JC, Wackernagel M, Galli A (2013) Accounting for demand and supply of the biosphere's regenerative capacity: The National Footprint Accounts' underlying methodology and framework. Ecol Ind 24:518–533

Brownlee J (2020) How to calculate precision, recall, and F-measure for imbalanced classification. https://machinelearningmastery.com/precision-recall-and-f-measure-for-imbalanced-classification/. Accessed 28 December 2020

Cao W, Yuan X (2019) Region-county characteristic of spatial-temporal evolution and influencing factor on land use-related CO2 emissions in Chongqing of China, 1997–2015. J Clean Prod 231:619–632

Caspersen JP, Pacala SW, Jenkins JC, Hurtt GC, Moorcroft PR, Birdsey RA (2000) Contributions of land-use history to carbon accumulation in US forests. Science 290(5494):1148–1151

Central Committee of the Communist Party of China (2019) Outline Development Plan for the Guangdong-Hong Kong-Macao Greater Bay Area. https://www.bayarea.gov.hk/filemanager/en/share/pdf/Outline_Development_Plan.pdf. Accessed 4 August 2020

Chapa F, Hariharan S, Hack J (2019) A new approach to high-resolution urban land use classification using open access software and true color satellite images. Sustainability 11(19):5266

Chen W, Ye X, Li J, Fan X, Liu Q, Dong W (2019a) Analyzing requisition–Compensation balance of farmland policy in China through telecoupling: a case study in the middle reaches of Yangtze River Urban Agglomerations. Land Use Policy 83:134–146

Chen Y, Li X, Liu X, Zhang Y, Huang M (2019b) Tele-connecting China's future urban growth to impacts on ecosystem services under the shared socioeconomic pathways. Sci Total Environ 652:765–779

Chen M, Vernon CR, Graham NT, Hejazi M, Huang M, Cheng Y, Calvin K (2020a) Global land use for 2015–2100 at 0.05° resolution under diverse socioeconomic and climate scenarios. Sci Data 7(1):1–11

Chen Y, Li X, Huang K, Luo M, Gao M (2020b) High-resolution gridded population projections for China under the shared socioeconomic pathways. Earth's Future 8(6):e2020EF001491

Chu L, Sun T, Wang T, Li Z, Cai C (2018) Evolution and prediction of landscape pattern and habitat quality based on CA-Markov and InVEST model in hubei section of three gorges reservoir area (TGRA). Sustainability 10(11):3854

Clark labs (2020) Land change modeler in Terrset. https://clarklabs.org/terrset/land-change-modeler/. Accessed 30 December 2020

DasGupta R, Hashimoto S, Okuro T, Basu M (2019) Scenario-based land change modelling in the Indian Sundarban delta: an exploratory analysis of plausible alternative regional futures. Sustain Sci 14(1):221–240

Department of Natural Resources of Guangdong Province (2017) Land planning of Guangdong Province (2016–2030). http://nr.gd.gov.cn/attachment/0/188/188208/506474.pdf. Accessed 23 November 2020

Department of Natural Resources of Guangdong Province (2018) Land Planning of Guangdong Province (2016–2035). http://nr.gd.gov.cn/attachment/0/187/187183/586580.pdf. Accessed 23 November 2020

Díaz S, Settele J, Brondízio E, Ngo H, Guèze M, Agard J, Arneth A, Balvanera P, Brauman K, Butchart S, Chan K, Garibaldi L, Ichii K, Liu J, Subramanian S, Midgley G, Miloslavich P, Molnár Z, Obura D, Pfaff A, Polasky S, Purvis A, Razzaque J, Reyers B, Chowdhury R, Shin Y, Visseren-Hamakers I, Willis K, and Zayas C (eds) (2020) Summary for policymakers of the global assessment report on biodiversity and ecosystem services of the Intergovernmental Science-Policy Platform on Biodiversity and Ecosystem Services. IPBES secretariat, Bonn, Germany. https://doi.org/10.5281/zenodo.3553579

Dong N, You L, Cai W, Li G, Lin H (2018) Land use projections in China under global socioeconomic and emission scenarios: Utilizing a scenario-based land-use change assessment framework. Glob Environ Chang 50:164–177

DSEC (2020) Statistical website of the Guangdong-Hong Kong-Macao Greater Bay Area. https://www.dsec.gov.mo/BayArea/en-US/#home. Accessed 8 December 2020

Eastman JR (2015) TerrSet manual. Clark University, Worcester

Eastman J, Toledano J (2018) A short presentation of the Land Change Modeler (LCM). In: Olmedo MTC, Paegelow M, Mas J-F, Escobar F (eds) Geomatic approaches for modeling land change scenarios. Springer, Cham, pp 499–505

Estoque RC, Ooba M, Avitabile V, Hijioka Y, DasGupta R, Togawa T, Murayama Y (2019) The future of Southeast Asia's forests. Nat Commun 10(1):1–12

Global footprint network (2019) Working guidebook to the national footprint and biocapacity accounts. https://www.footprintnetwork.org/content/uploads/2019/05/National_Footprint_Accounts_Guidebook_2019.pdf. Accessed 28 August 2020

Global footprint network (2020a) Glossary. https://www.footprintnetwork.org/resources/glossary/. Accessed 1 January 2021

Global footprint network (2020b) Open data platform. https://data.footprintnetwork.org/?_ga=2.62753900.1324893541.1611108161-1081994963.1587799037#/. Accessed 20 January 2021

Gomes L, Bianchi F, Cardoso I, Schulte R, Arts B, Fernandes Filho E (2020) Land use and land cover scenarios: an interdisciplinary

approach integrating local conditions and the global shared socioeconomic pathways. Land Use Policy 97:104723

Greater Bay Area (2018) Overview. https://www.bayarea.gov.hk/en/about/overview.html. Accessed 3 August 2020

Gu X (2019) Agricultural cooperation and development in Guangdong-Hong Kong-Macao Great Bay Area: status quo, problems and countermeasures. J Political Sci Law 4:5–7

Gu B, Zhang X, Bai X, Fu B, Chen D (2019) Four steps to food security for swelling cities. Nature Publishing Group, Berlin

Han L, Meng P, Jiang R, Xu B, Zhang B, Chen M (2018) Logical root, pattern exploration and management innovation of balancing cultivated land occupation and reclamation in the new era. China Land Sci 32(6):90–96

Hasan S, Shi W, Zhu X, Abbas S, Khan HUA (2020) Future simulation of land use changes in rapidly urbanizing south china based on land change modeler and remote sensing data. Sustainability 12(11):4350

Hashimoto S, DasGupta R, Kabaya K, Matsui T, Haga C, Saito O, Takeuchi K (2019) Scenario analysis of land-use and ecosystem services of social-ecological landscapes: implications of alternative development pathways under declining population in the Noto Peninsula. Jpn Sustain Sci 14(1):53–75

Hausfather Z (2018) Explainer: How 'Shared Socioeconomic Pathways' explore future climate change. https://www.carbonbrief.org/explainer-how-shared-socioeconomic-pathways-explore-future-climate-change. Accessed 19 August 2020

He C, Li J, Zhang X, Liu Z, Zhang D (2017) Will rapid urban expansion in the drylands of northern China continue: a scenario analysis based on the land use scenario dynamics-urban model and the shared socioeconomic pathways. J Clean Prod 165:57–69

Hewitt RJ, Compagnucci AB, Castellazzi M, Dunford RW, Harrison PA, Pedde S, Gimona A (2020) Impacts and trade-offs of future land use and land cover change in Scotland: spatial simulation modelling of shared socioeconomic pathways at regional scales. https://doi.org/10.31235/osf.io/fc6he

Houghton RA, House J, Pongratz J, Van Der Werf G, DeFries R, Hansen M, Le Quéré C, Ramankutty N (2012) Carbon emissions from land use and land-cover change. Biogeosciences 12:5125–5142

IIASA (2018) SSP database version 2.0. https://tntcat.iiasa.ac.at/SspDb/dsd?Action=htmlpage&page=welcome. Accessed 3 September 2020

IPBES (2016a) Methodological assessment report on scenarios and models of biodiversity and ecosystem services—summary for policymakers. https://ipbes.net/sites/default/files/downloads/pdf/spm_deliverable_3c_scenarios_20161124.pdf. Accessed 30 August 2020

IPBES (2016b) Scenarios and models: new scenarios and supporting assessments. https://ipbes.net/scenarios-models. Accessed 30 August 2020

IPBES (2020) IPBES-IPCC co-sponsored workshop: spotlighting the interactions of the science of biodiversity and climate change. https://ipbes.net/ipbes-ipcc-cosponsored-workshop-media-release. Accessed 4 January 2021

Jiao M, Hu M, Xia B (2019) Spatiotemporal dynamic simulation of land-use and landscape-pattern in the Pearl River Delta, China. Sustain Cities Soc 49:101581

Jones B, O'Neill BC (2016) Spatially explicit global population scenarios consistent with the Shared Socioeconomic Pathways. Environ Res Lett 11(8):084003

Kindu M, Schneider T, Döllerer M, Teketay D, Knoke T (2018) Scenario modelling of land use/land cover changes in Munessa-Shashemene landscape of the Ethiopian highlands. Sci Total Environ 622:534–546

Kok K, Pedde S, Gramberger M, Harrison PA, Holman IP (2019) New European socio-economic scenarios for climate change research: operationalising concepts to extend the shared socio-economic pathways. Reg Environ Change 19(3):643–654

Kumar KS, Bhaskar PU, Padmakumari K (2015) Application of land change modeler for prediction of future land use land cover: a case study of Vijayawada City. Int J Adv Technol Eng Sci 3(1):773–783

Leung D, Newsam S (2012) Exploring geotagged images for land-use classification. In: Proceedings of the ACM multimedia 2012 workshop on Geotagging and its applications in multimedia pp 3–8

Li X, Chen Y (2020) Projecting the future impacts of China's cropland balance policy on ecosystem services under the shared socioeconomic pathways. J Clean Prod 250:119489

Li J, Wang J (2019) Identification, classification, and mapping of coastal ecosystem services of the Guangdong, Hong Kong, and Macao Great Bay Area. Acta Ecol Sin 9(17):6393–6403. https://doi.org/10.5846/stxb201805231130

Li X, Yu L, Sohl T, Clinton N, Li W, Zhu Z, Liu X, Gong P (2016) A cellular automata downscaling based 1 km global land use datasets (2010–2100). Sci Bull 61(21):1651–1661

Li X, Zhou Y, Eom J, Yu S, Asrar GR (2019) Projecting global urban area growth through 2100 based on historical time series data and future Shared Socioeconomic Pathways. Earth's Future 7(4):351–362

Liao W, Liu X, Xu X, Chen G, Liang X, Zhang H, Li X (2020) Projections of land use changes under the plant functional type classification in different SSP-RCP scenarios in China. Sci Bull 65:1935

Lin W, Sun Y, Nijhuis S, Wang Z (2020) Scenario-based flood risk assessment for urbanizing deltas using future land-use simulation (FLUS): Guangzhou Metropolitan Area as a case study. Sci Total Environ 739:139899

Liu M, Li W, Xie G (2010) Estimation of China ecological footprint production coefficient based on net primary productivity. Chin J Ecol 29(3):592–597

Liu X, Liang X, Li X, Xu X, Ou J, Chen Y, Li S, Wang S, Pei F (2017) A future land use simulation model (FLUS) for simulating multiple land use scenarios by coupling human and natural effects. Landsc Urban Plan 168:94–116

Liu X, Huang Y, Xu X, Li X, Li X, Ciais P, Lin P, Gong K, Ziegler AD, Chen A (2020) High-spatiotemporal-resolution mapping of global urban change from 1985 to 2015. Nat Sustain 3:1–7

Lu Y, Wu P, Ma X, Li X (2019) Detection and prediction of land use/land cover change using spatiotemporal data fusion and the Cellular Automata–Markov model. Environ Monit Assess 191(2):68

Lundquist CJ, Pereira HM, Porto CADV, Peterson GD, Karlsson-Vinkhuyzen S, Pereira L, Acosta LA, Akcakaya HR, Davies KK, Den Belder E (2020) A pluralistic Nature Futures Framework. https://edisciplinas.usp.br/pluginfile.php/4884426/mod_resource/content/1/Relat%C3%B3rio%20IPBES.pdf. Accessed 24 July 2021

Mallapaty S (2020) How China could be carbon neutral by mid-century. Nature 586(7830):482–483

Mas J, Paegelow M, Olmedo MC (2018) LUCC modeling approaches to calibration. Geomatic approaches for modeling land change scenarios. Springer, Cham, pp 11–25

Mohammady M, Moradi H, Zeinivand H, Temme A (2015) A comparison of supervised, unsupervised and synthetic land use classification methods in the north of Iran. Int J Environ Sci Technol 12(5):1515–1526

Moran DD, Wackernagel M, Kitzes JA, Goldfinger SH, Boutaud A (2008) Measuring sustainable development—Nation by nation. Ecol Econ 64(3):470–474

Nakicenovic N, Lempert RJ, Janetos AC (2014) A framework for the development of new socio-economic scenarios for climate change research: introductory essay. Clim Change 122(3):351–361

Nilsson AE, Bay-Larsen I, Carlsen H, van Oort B, Bjørkan M, Jylhä K, Klyuchnikova E, Masloboev V, van der Watt L-M (2017) Towards extended shared socioeconomic pathways: a combined participatory bottom-up and top-down methodology with results from the Barents region. Glob Environ Chang 45:124–132

O'Neill BC, Kriegler E, Ebi KL, Kemp-Benedict E, Riahi K, Rothman DS, van Ruijven BJ, van Vuuren DP, Birkmann J, Kok K (2017) The roads ahead: narratives for shared socioeconomic pathways describing world futures in the 21st century. Glob Environ Chang 42:169–180

O'Neill BC, Carter TR, Ebi K, Harrison PA, Kemp-Benedict E, Kok K, Kriegler E, Preston BL, Riahi K, Sillmann J (2020) Achievements and needs for the climate change scenario framework. Nat Clim Change 10:1–11

Olmedo MC, Mas J (2018) Markov CHAIN. Geomatic approaches for modeling land change scenarios. Springer, Cham, pp 441–445

Palazzo A, Vervoort JM, Mason-D'Croz D, Rutting L, Havlík P, Islam S, Bayala J, Valin H, Kadi HAK, Thornton P (2017) Linking regional stakeholder scenarios and shared socioeconomic pathways: quantified West African food and climate futures in a global context. Glob Environ Chang 45:227–242

People's government of Guangdong province (2019) Issuance of the work plan for the compilation of land planning of Guangdong Province (2020–2035). http://www.gd.gov.cn/zwgk/zcjd/snzcsd/content/post_2530532.html. Accessed 30 December 2020 (in Chinese)

People's government of Guangdong province (2020) The Ministry of Natural Resources issued nine guidelines to support the Greater Bay Area and Shenzhen in exploring the reform of natural resources, and Guangdong province in exploring the built-up land trading mechanism on the provincial scale. http://www.gd.gov.cn/gdywdt/gdyw/content/post_3058085.html. Accessed 13 October 2020 (in Chinese)

Pereira LM, Davies KK, den Belder E, Ferrier S, Karlsson-Vinkhuyzen S, Kim H, Kuiper JJ, Okayasu S, Palomo MG, Pereira HM (2020) Developing multiscale and integrative nature–people scenarios using the Nature Futures Framework. People Nat 2:1172

Popp A, Calvin K, Fujimori S, Havlik P, Humpenöder F, Stehfest E, Bodirsky BL, Dietrich JP, Doelmann JC, Gusti M (2017) Land-use futures in the shared socio-economic pathways. Glob Environ Chang 42:331–345

Rawat J, Kumar M (2015) Monitoring land use/cover change using remote sensing and GIS techniques: a case study of Hawalbagh block, district Almora, Uttarakhand, India. Egypt J Remote Sens Space Sci 18(1):77–84

Riahi K, Van Vuuren DP, Kriegler E, Edmonds J, Oneill BC, Fujimori S, Bauer N, Calvin K, Dellink R, Fricko O (2017) The shared socioeconomic pathways and their energy, land use, and greenhouse gas emissions implications: an overview. Glob Environ Change 42:153–168

Rimal B, Zhang L, Keshtkar H, Haack BN, Rijal S, Zhang P (2018) Land use/land cover dynamics and modeling of urban land expansion by the integration of cellular automata and markov chain. ISPRS Int J Geo Inf 7(4):154

Ritchie H, Roser M (2017) CO2 and greenhouse gas emissions. https://ourworldindata.org/greenhouse-gas-emissions Accessed 19 January 2021

Rosa IM, Pereira HM, Ferrier S, Alkemade R, Acosta LA, Akcakaya HR, Den Belder E, Fazel AM, Fujimori S, Harfoot M (2017) Multiscale scenarios for nature futures. Nat Ecol Evol 1(10):1416–1419

Rosa I, Lundquist CJ, Ferrier S, Alkemade R, Castro PF, Joly CA (2020) Increasing capacity to produce scenarios and models for biodiversity and ecosystem services. Biota Neotropica 20 (suppl 1). https://doi.org/10.1590/1676-0611-BN-2020-1101

Ruben GB, Zhang K, Dong Z, Xia J (2020) Analysis and projection of land-use/land-cover dynamics through scenario-based simulations using the CA-markov model: a case study in Guanting Reservoir Basin, China. Sustainability 12(9):3747

Saito O, Kamiyama C, Hashimoto S, Matsui T, Shoyama K, Kabaya K, Uetake T, Taki H, Ishikawa Y, Matsushita K (2019) Co-design of national-scale future scenarios in Japan to predict and assess natural capital and ecosystem services. Sustain Sci 14(1):5–21

Saxena S (2018) Precision vs recall. https://medium.com/@shrutisaxena0617/precision-vs-recall-386cf9f89488. Accessed 28 December 2020

ScienceNet.cn (2019) How to develop the eco-agricultural pathway in the Greater Bay Area. http://news.sciencenet.cn/sbhtmlnews/2019/7/348220.shtm?id=348220. Accessed 13 October 2020 (in Chinese)

Shi H, Mu X, Zhang Y, Lv M (2012) Effects of different land use patterns on carbon emission in Guangyuan city of Sichuan province. Bull Soil Water Conserv 32(3):101–106 (**in Chinese**)

Shi X, Matsui T, Machimura T, Gan X, Hu A (2020) Toward sustainable development: decoupling the high ecological footprint from human society development: a case study of Hong Kong. Sustainability 12(10):4177

Shoyama K, Matsui T, Hashimoto S, Kabaya K, Oono A, Saito O (2019) Development of land-use scenarios using vegetation inventories in Japan. Sustain Sci 14(1):39–52

Solecki WD, Oliveri C (2004) Downscaling climate change scenarios in an urban land use change model. J Environ Manage 72(1–2):105–115

Song S, Liu Z, He C, Lu W (2020) Evaluating the effects of urban expansion on natural habitat quality by coupling localized shared socioeconomic pathways and the land use scenario dynamics-urban model. Ecol Indic 112:106071

Tang H, Sang L, Yun W (2020) China's cultivated land balance policy implementation dilemma and direction of scientific and technological innovation. Bull Chin Acad Sci 35(5):637–644. https://doi.org/10.16418/j.issn.1000-3045.20200313002

The Environmental Protection Department of Hong Kong (2017) Hong Kong greenhouse gas inventory for 2015 released. https://www.info.gov.hk/gia/general/201707/10/P2017071000628.htm?fontSize=1. Accessed 1 January 2021

The National People's Congress of the PRC (2019) Land Administration Law of the PRC. http://www.npc.gov.cn/npc/c30834/201909/d1e6c1a1eec345eba23796c6e8473347.shtml. Accessed 13 October 2020 (in Chinese)

United States Environmental Protection Agency (2018) Overview of greenhouse gases. https://www.epa.gov/ghgemissions/overview-greenhouse-gases. Accessed 19 January 2021

Valdivia RO, Antle JM, Rosenzweig C, Ruane AC, Vervoort J, Ashfaq M, Hathie I, Tui SH-K, Mulwa R, Nhemachena C (2015) Representative agricultural pathways and scenarios for regional integrated assessment of climate change impacts, vulnerability, and adaptation. Handb Clim Change Agroecosyst 3:101–156

Van Ruijven BJ, Levy MA, Agrawal A, Biermann F, Birkmann J, Carter TR, Ebi KL, Garschagen M, Jones B, Jones R (2014) Enhancing the relevance of shared socioeconomic pathways for climate change impacts, adaptation and vulnerability research. Clim Change 122(3):481–494

van Vliet J (2019) Direct and indirect loss of natural area from urban expansion. Nat Sustain 2(8):755–763

Vázquez-Quintero G, Solís-Moreno R, Pompa-García M, Villarreal-Guerrero F, Pinedo-Alvarez C, Pinedo-Alvarez A (2016) Detection and projection of forest changes by using the Markov Chain Model and cellular automata. Sustainability 8(3):236

Wackernagel M, Rees WE (1996) Our ecological footprint: reducing human impact on the Earth. New Society Publishers, Gabriola Island

Wan J, Han Y (2019) Inter-regional comparison of edible agricultural product supply capability and agricultural industrial chain function in the Greater Bay Area. J South China Univ Technol (soc Sci Ed) 21(6):9–20. https://doi.org/10.19366/j.cnki.1009-055X.2019.06.002

Wang L, Yang Y, Feng Z, You Z (2014) Prediction of China's population in 2020 and 2030 on county scale. Geogr Res 33(2):310

Wang R, Derdouri A, Murayama Y (2018) Spatiotemporal simulation of future land use/cover change scenarios in the Tokyo metropolitan area. Sustainability 10(6):2056

Wang C, Wang Y, Wang R, Zheng P (2018) Modeling and evaluating land-use/land-cover change for urban planning and sustainability: a case study of Dongying city, China. J Clean Prod 172:1529–1534

Worldpop (2020) Population counts-individual countries 2000–2020 UN adjusted (100m resoultion). https://www.worldpop.org/geodata/listing?id=69. Accessed 28 August 2020

WWF (2013) Hong Kong ecological footprint report 2013. https://www.footprintnetwork.org/content/images/article_uploads/hong_kong_ecological_footprint_report_2013.pdf. Accessed 9 December 2020

WWF (2019) Guangdong-Hong Kong-Macao Greater Bay Area Ecological Footprint Report. http://www.wwf-opf.org.cn/upload/news/609b9697e4abe961e224e401852e41f2.pdf. Accessed 13 October 2020 (in Chinese)

Yang G, Zhu W, Wen Y, Lin Y (2019) Spatial differentiation in the intensify and efficiency of carbon emission from land use in Guangdong province in past two decades. Ecol Environ Sci 28(2):332–340 ((in Chinese))

Yang B, Chen X, Wang Z, Li W, Zhang C, Yao X (2020) Analyzing land use structure efficiency with carbon emissions: a case study in the Middle Reaches of the Yangtze River, China. J Clean Prod 274:123076

Yirsaw E, Wu W, Shi X, Temesgen H, Bekele B (2017) Land use/land cover change modeling and the prediction of subsequent changes in ecosystem service values in a coastal area of China, the Su-Xi-Chang Region. Sustainability 9(7):1204

Zhang R, Matsushima K, Kobayashi K (2018) Can land use planning help mitigate transport-related carbon emissions? A case of Changzhou. Land Use Policy 74:32–40

Zhu Y, Deng X, Newsam S (2019) Fine-grained land use classification at the city scale using ground-level images. IEEE Trans Multimedia 21(7):1825–1838

**Publisher's Note** Springer Nature remains neutral with regard to jurisdictional claims in published maps and institutional affiliations.